Contents lists available at ScienceDirect

Arabian Journal of Chemistry

journal homepage: www.ksu.edu.sa

Exploring the essence of celery seeds (*Apium graveolens* L.): Innovations in microwave-assisted hydrodistillation for essential oil extraction using *in vitro*, *in vivo* and *in silico* studies

Ghizlane Nouioura [a,*], Mohamed El fadili [b], Hazem K. Ghneim [c], Latifa Zbadi [d], Souad Maache [a], Otmane Zouirech [a], Mohamed Danouche [e], Mourad A.M. Aboul-Soud [c], John P. Giesy [f,g,h], Badiaa Lyoussi [a], Elhoussine Derwich [a,i]

[a] *Laboratory of Natural Substances, Pharmacology, Environment, Modeling, Health and Quality of Life (SNAMOPEQ), Faculty of Sciences Dhar El-Mehraz, Sidi Mohamed Ben Abdellah University, Fez 30 000, Morocco*
[b] *LIMAS Laboratory, Faculty of Sciences Dhar El Mehraz, Sidi Mohammed Ben Abdellah University, Fez, Morocco*
[c] *Department of Clinical Laboratory Sciences, College of Applied Medical Sciences, King Saud University, P.O. Box 10219, Riyadh 11433, Saudi Arabia*
[d] *Public Health Laboratories at the Prefectural Delegation of Tangier Assilah, Tangier, Morocco*
[e] *Departement of Chemical & Biochemical Sciences-Green Process Engineering (CBS-GPE), Mohammed VI Polytechnic University (UM6P), Benguerir, Morocco*
[f] *Department of Environmental Sciences, Baylor University, Waco, TX 76798, USA*
[g] *Department of Veterinary Biomedical Sciences and Toxicology Centre, University of Saskatchewan, Saskatoon, SK S7N 5B3, Canada*
[h] *Department of Integrative Biology and Integrative Toxicology Program, Michigan State University, East Lansing, MI 48824, USA*
[i] *Unity of GC/MS and GC, City of Innovation, Sidi Mohamed Ben Abdellah University, Fez, Morocco*

A R T I C L E I N F O

Keywords:
A. graveolens
Microwave-assisted hydro-distillation
Essential oil
Chemical composition
Pharmaceutical drugs
PASS prediction

A B S T R A C T

This study presents the composition analysis of essential oils extracted from celery seeds (*Apium graveolens* L.) collected from Morocco. Essential oil of *A. graveolens* (AG-EO), were obtained through microwave-assisted hydro-distillation, and its composition was characterized using gas chromatography/mass spectrometry (GC/MS). antimicrobial properties were assessed utilizing disc diffusion and microdilution assay methods, while antioxidant activities were evaluated through spectrophotometric techniques. Additionally, *in vivo* anti-inflammatory effects were investigated. The molecular docking technique, a computational approach utilized to predict the binding of small molecules to specific proteins, was employed to elucidate the antioxidative and antibacterial characteristics of the constituent molecules. The physicochemical and pharmacokinetic features of absorption, distribution, metabolism, excretion, and toxicity (ADME-Tox) tests were anticipated to provide insights into the drug likeness, pharmacokinetic characteristics, and expected safety profiles upon ingestion and the potential pharmacological activity of the identified compounds. Fifteen constituent compounds representing 99.99% of AG-EO were identified and quantified by the use of GC/MS. The main constituent, comprising 64.58% of AG-EO was limonene. AG-EO demonstrated a significant DPPH free radical scavenging activity, showing estimated scavenging rates of 8.49±0.00 μg/mL, and 5.09±0.04 μg/mL for $ABTS^{+}$. AG-EO exhibited reducing Power (RP) and total antioxidant activity (TAC) of 3.42±0.01 μg/mL and 245.93±0.04 mg AAE/mL, respectively. AG-EO exhibited significant antimicrobial activity against all tested microorganisms. Additionally, the anti-inflammatory activity demonstrated the remarkable efficacy of AG-EO. Taken together, the essential oil derived from celery seeds holds promise for large-scale utilization as an environmentally friendly preservative within the food and agriculture industries, effectively countering fungal growth and aflatoxin contamination in stored commodities. Additionally, it exhibits potential as a suitable candidate for the development of pharmaceutical drugs.

* Corresponding author.
E-mail address: ghizlane.nouioura@usmba.ac (G. Nouioura).

https://doi.org/10.1016/j.arabjc.2024.105726
Received 9 January 2024; Accepted 10 March 2024
Available online 11 March 2024

1. Introduction

Conventional therapies and the use of plants in empirical medicine have often been the sources of high-level scientific research (Nouioura et al., 2023a,b). This research often leads to discoveries of novel substances useful as therapeutics. The majority of these compounds are secondary metabolites that are typically produced by plants as a protective mechanism against physical or biological invaders, such as insects, microbes, and herbivores. (Ayman et al., 2008).

Essential oils (EOs), sometimes referred to as "volatile oils," are complex mixtures of volatile or semi-volatile constituent chemicals produced by aromatic plants as secondary metabolites and are responsible for the characteristics of aromatic plants such as their powerful aromas (Ben Abada et al., 2020). EOs are generally fluid, volatile, and soluble in lipids and organic solvents. They can be present in all portions of plants, including roots, seeds, buds, flowers, leaves, stems, fruits, wood, or bark. EOs exhibit diverse compositions of bioactive components, primarily consisting of terpenoids, monoterpenes, and sesquiterpenes (Tohidi et al., 2017). Biological effects of EOs are caused by interactions of these bioactive substances with biomolecules (Tosun et al., 2023). For instance, mono-terpenoids specifically interfere with physiological and biochemical procedures associated with growth and expansion of microorganisms, affecting and modulating their proliferation and development (Bat-Özmatara, 2020). Extraction methods, including steam distillation, solvent extraction, and supercritical fluid extraction have been applied to extract EOs (Majda et al., 2020). Microwave-assisted extraction (MHD) is a technique used for extracting valuable compounds from plant materials, which can be tailored to suit extractions on a small or large scale. MHD exhibits outstanding performance in terms of both the quantity and quality of the oils extracted, as well as time and cost efficiency. Additionally, it effectively minimizes energy consumption and reduces the emission of carbon dioxide into the atmosphere. As a result, MHD has gained significant popularity and is extensively utilized in both laboratory and industrial settings (Moradi, Fazlali, et Hamedi 2018). Other key features include rapid energy transfer, efficient heating, and an environmentally eco-friendly isolation system (Zhang, Yang, et Wang 2011).

Celery and its essential oil (AG-EO) are renowned for their therapeutic, medicinal, and industrial properties (Modaresi, Ghalamkari, et Jalalizand 2012). Due to its antimicrobial properties against mold, yeast, and bacteria, as well as its antioxidant properties, AG-EO might be an alternative natural preservative and nutraceutical ingredients (Liu et al., 2021).

The purpose of this study was to enhance the EO yield by utilizing microwave-assisted distillation of celery seeds. The biochemical components of Moroccan EO of celery (*A. graveolens*) were analyzed using GC–MS/MS and selected *in vitro* and PASS prediction with *in silico* assays were employed to evaluate antioxidant activities such as DPPH, ABTS, RP, and TAC, as well as the anti-inflammatory, and the antimicrobial activity against multi-resistant pathogenic microorganisms. The results of this study are presented here to showcase the improvements achieved.

2. Materials and methods

2.1. Plant material

Seeds of *Apium graveolens* L. were gathered from the town of Sefrou in June 2022. A voucher specimen has been meticulously cataloged and deposited at the Laboratory of Natural Substances, Pharmacology, Environment, Modeling, Health, and Quality of Life (SNAMOPEQ), situated within the Faculty of Sciences at Dhar El-Mehraz, Sidi Mohamed Ben Abdellah University, herbarium under the designated number RAB38370. Following collection, the seeds were meticulously processed by pulverization utilizing a professional herb grinder (Omni mixer 17106, Du Pont Company, USA). The resultant powder was carefully packed into glass bottles, and all samples were safeguarded at ambient temperature until the moment of essential oil extraction.

2.2. Microwave-assisted hydrodistillation of the volatile oil

The quantitative composition, physicochemical properties, and biological activity of the essential oil extracted from the raw material, isolated under optimal parameters, were subjected to comprehensive analysis. The MHD process was conducted with the use of a microwave oven as the power source, specifically the MWD 119 WH, Whirlpool, China, which had a 20 L capacity and operated at 2.45 GHz frequency. The microwave oven was directly connected to a Clevenger apparatus, and it featured a cooling system for continuous condensation of the distillate. The microwave oven operated at 1,100 Watts while producing 700 Watts, with a power source of 230 V at 50 Hz and cavity dimensions of 216 x 302 x 277 mm.

For the extraction process, 100 g of ground celery seeds were combined with 1 L of water in a 2-liter flask and heated inside the microwave oven cavity at 600 W for 30 min. The vapor mixture of water and essential oil was continuously condensed in an external cooling system connected to the microwave cavity, and the recovered distillate was collected in a Clevenger receiver. To maintain constant humidity conditions during the extraction process, excess condensed water was refluxed back into the extraction flask (Majda et al., 2020).

Following the extraction process, the EOs were collected, dehydrated by adding anhydrous sodium sulfate, weighed, and stored in a vial at 4 °C in the dark.

2.3. Chemical characterization of essential oil by GC/MS

The chemical constituents of the EO were identified and quantified using gas chromatography, specifically the TRACE GC-ULTRA (Serial Number: 20062969) by Thermo-Fisher Scientific in Waltham, MA, USA, coupled with mass spectrometry, utilizing the Quadrapole (Serial Number: 210729) also by Thermo-Fisher Scientific. The analysis employed a capillary column (HP-5MS) with a length of 50 m, an internal diameter of 0.32 mm, and a film thickness of 1.25 μm.

The temperature was programmed to increase from 40 °C to 280 °C at a rate of 5 °C per minute. The injector and detector (Polaris Q) temperatures were set at 250 °C and 200 °C, respectively. Ionization was achieved using the electron-impact mode (EI) at 70 eV. Helium was used as the carrier gas, with a flow rate of 1 mL/min and a split ratio of 1:40. For the analysis, 1 Âμl of EO was injected.

To identify and quantify the components, retention times were compared with those stored in the NIST-MS Search Version 2.0 library, and the percentages of each constituent were calculated. Components were subsequently identified through this process.

2.4. Antioxidant activity of AG-EO

2.4.1. DPPH scavenging capacity

Free radical scavenging activity against the 1,1-diphenyl-2-picrylhydrazyl (DPPH) radical was evaluated using previously described methods (Nouioura et al., 2023a,b). A volume of 50 μL of EO, dissolved in ethanol was used at different concentrations and mixed with 825 μL of DPPH. The reaction mixture was allowed to stand in the dark for 60 min, then absorbance was measured at 517 nm. BHT (Butylated hydroxytoluene) was used as a standard. All determinations were performed in triplicate. Using the following equation, the IC_{50} values were determined from the graph by the % inhibition (Equation 1).

$$\text{Inhibition}\,(\%) = \frac{\text{Abs control} - \text{Abs sample}}{\text{Abs control}} \times 100 \quad (1)$$

2.4.2. ABTS radical scavenging activity

Free radical scavenging activity of AG-EO was determined by use of an ABTS free radical cation decolorization assay (Re et al., 1999). In

summary, 50 µL of various dilutions of each ethanolic extract, as well as BHT utilized as a positive control, were combined with 825 µL of the ABTS radical cation solution. These solutions were incubated in the dark for 6 min at room temperature. Subsequently, the absorbance measurements were recorded at 734 nm using a UV/Vis spectrophotometer.

A blank sample containing an equivalent amount of ethanol and ABTS solution was used as a negative control for reference. The percentage inhibition of absorbance was calculated using Equation 1, and the IC_{50} (half-maximal inhibitory concentration) values were graphically determined and expressed in micrograms per milliliter (µg/mL). All analyses were conducted in triplicate.

2.4.3. Reducing power (RP)

The determination of reducing power was conducted following established procedures (Oyaizu, 1986). Specifically, a volume of 50 µL of AG-EO was combined with 200 µL of 0.2 M sodium phosphate buffer (pH 7.6) and 200 µL of 1 % potassium ferricyanide. The mixture was then incubated at 50 °C for 20 min to facilitate the conversion of ferricyanide to ferrocyanide. Subsequently, 200 µL of 10 % trichloroacetic acid was added to terminate the reaction. The mixture was centrifuged at a force of 500 g for 10 min. Finally, the supernatant was mixed with 600 µL of distilled water and 120 µL of 0.1 % ferric chloride. A linear relationship was established by plotting absorbance at 700 nm against sample concentration. The results were defined as the concentration of the extract at which the absorbance reached 0.5 (EC_{50}) and were expressed in µg/mL. Each experiment was conducted in triplicate. An increase in absorbance in the reaction mixture signifies an enhancement in reducing power. Ascorbic acid was used as a positive control at various concentrations.

2.4.4. Total antioxidant activity (TAC)

The total antioxidant capacities (TAC) of all extracts were assessed using the phosphomolybdenum method as outlined by Nouioura et al., 2023a,b. In this procedure, fifty microliters of AG-EO or a standard reference substance (Ascorbic acid) were mixed with 1 mL of a reagent solution composed of 0.6 M sulfuric acid, 28 mM sodium phosphate, and 4 mM ammonium molybdate. The absorbance of the sample was measured at 695 nm after 90 min of incubation in a water bath at 95 °C, utilizing a PerkinElmer Lambda 40 UV/Vis spectrophotometer, and this measurement was compared to a blank. The results were expressed as milligrams of ascorbic acid equivalent (mg AAE) per gram of EO (mg AAE/g EO) and were reported as the mean of three triplicate measurements ± standard deviation (SD). Quercetin and BHT were employed as standards in this analysis.

2.5. Antimicrobial activity of AG-EO

2.5.1. Microbial strains tested

The antimicrobial testing of AG-EO was conducted on various microorganisms, including Gram-positive bacteria (*Bacillus subtilis* DSM 6333 and *Staphylococcus aureus* ATCC 6633), Gram-negative bacteria (*Proteus mirabilis* ATCC 29.906), and a fungal strain (*Candida albicans* ATCC 10.231). These microorganisms were selected based on their common occurrence as contaminants in food products and their pathogenic nature. The bacterial strains were obtained and identified at the bacteriology laboratory of Hassan II Hospital in Fez, Morocco. For the yeast strain, it was inoculated on Sabouraud dextrose agar, while the bacterial strains were streaked on Mueller-Hinton agar. Bacterial cultures were incubated for 18–24 h at 37 °C, and the yeast culture was incubated at 30 °C for the same duration. To prepare the test suspensions, well-isolated colonies were selected and emulsified in 10 mL of physiological water buffered with 0.9 % phosphate and sterilized. Dilutions were performed to standardize the bacterial suspension to a 0.5 McFarland turbidity standard.

2.5.2. Disc method for AG-EO

The antimicrobial efficacy of AG-EO was assessed using the disk diffusion method as described by El Barnossi et al. in 2020, for both bacteria and fungi. In this approach, 6 mm-diameter sterilized Whatman paper discs were impregnated with AG-EO at a volume of 10 µL per disc and then placed on the surface of Mueller Hinton Agar (MHA)-coated agar medium, which had previously been inoculated with a microbial suspension of the tested microorganism at a volume of 100 µL per 5 mL of MHA. To compare the effectiveness of AG-EO against bacteria and fungi, negative and positive controls were used. The positive controls included Oxacillin and Cefuroxime (10 µg/disc) for bacteria, and Fluconazole (10 µg/disc) for fungi. After an incubation period of 15–30 min at room temperature, the dishes were placed under specific conditions for yeast (30°C for 48h) and bacteria (37°C for 18–24h). Measurements of inhibition zone diameters in millimeters were used to determine inhibition percentages. Each test was conducted in triplicate, and the results were expressed as means ± standard deviation (SD) of triplicate measurements.

2.5.3. Determination of minimum inhibitory concentration (MIC)

The MIC of the AG-EO against the microorganisms was determined by use of the serial agar dilution method (Balouiri, Sadiki, et Ibnsouda 2016). Briefly microplates were made under aseptic conditions; each sterile 96-well microplate was labeled, and then a volume of 50 µL of AG-EO in 2% DMSO was pipetted into the first column of the plate; in all other wells, 50 µL of sterile Mueller-Hinton for bacterial strains and 40 µL of sterile EM for fungal strains were added; serial dilutions were made using after a 24-hour incubation period for bacteria and 48h for *C. albicans* at 37°C and 30°C, respectively. The MIC endpoint is determined using the colorimetric method (TTC 0.2 % (w/v)) (Balouiri et al., 2016).

2.6. In vivo anti-inflammatory activity

2.6.1. Animal handling and housing

Rats, both male and female, weighing 150–250 g, were obtained from the Sidi Mohamed Ben Abdellah University, Fez, animal facilities. Throughout their acclimatization period, the rats had unrestricted access to food and tap water, and their environment was meticulously controlled to maintain a temperature of 25 ± 1 °C and a photoperiod of 12 h (12 L/12 D).

The ethics committee of Sidi Mohamed Ben Abdallah University Mohammed, Fez, approved the experimental protocols, which followed the guidelines provided in the Declaration of Helsinki. The study was approved by the Laboratory of Natural Substances, Pharmacology, Environment, Modeling, Health, and Quality of Life at the Faculty of Science Dhar Mahraz in Fez, Morocco, with reference number USMBA-SNAMOPEQ 2023-03.

2.6.2. Carrageenan-induced rat paw inflammation

To investigate the anti-inflammatory activity of AG-EO we followed the protocol described in the study conducted by Winter et al., with slit modification (Mssillou et al., 2022). Wistar rats were divided into 5 groups (5 rats in each group). The first group (negative control) received only physiological water (0.9 % NaCl). Groups 2, and 3 treated with 1.5 mL/Kg, and 5 mL/Kg, respectivement of AG-EO vegetable oil. Group 3 used as a standard, received indomethacin® (LAPROPHAN, Casablanca, Morocco) orally (10 mg/kg). The circumference of the right paw of all rats was measured before the injection of carrageenan (1%); then the measurement was performed after 3, 4, 5, and 6 h of the injection. The percentage inhibition of inflammation was calculated according to the equation below:

$$PI\% = \frac{(Ct - C0)control - (Ct - C0)treated}{(Ct - C0)control} \times 100$$

Table 1
Phytochemical constituents contained in the essential oil extracted from Moroccan *Apium graveolens* (AG-Eo).

No	RT (min)	Molecular Formula	Compounds	RI		Peak Area %
				Cal	Lit	
1	1.72	$C_{10}H_{16}$	β-pinene	970	979	1.53
2	2.97	$C_{10}H_{16}$	limonene	1014	1029	64.58
3	6.10	$C_{10}H_{16}O$	limonene oxide	1130	1137	0.15
4	6.44	$C_{10}H_{16}O$	*cis*-Verbenol	1137	1141	0.53
5	6.69	$C_{11}H_{18}$	pentylcyclohexa-1,3-diene	1158	1161	0.08
6	17.49	$C_{10}H_{8}$	naphthalene	1177	1181	6.30
7	18.86	$C_{15}H_{24}$	β-humulene	1431	1439	0.19
8	17.91	$C_{15}H_{24}$	α-himachalene	1445	1451	1.88
9	20.05	$C_{15}H_{24}$	β-caryophyllene	1460	1466	0.26
10	20.96	$C_{15}H_{24}$	β-selinene	1481	1490	0.31
11	21.29	$C_{15}H_{26}O$	α-eudesmol	1645	1653	0.47
12	21.59	$C_{13}H_{16}O_3$	hexenyl salicylat	1659	1669	7.27
13	22.12	C_8H_7NO	2-methyl-benzoxazole	1700	1706	1.06
14	22.62	$C_{12}H_{16}O_2$	sedanenolide	1713	1720	15.38
			Chemical classes			
			Oxygenated monoterpenes			0.68
			Monoterpene hydrocarbons			72.41
			Oxygenated sesquiterpenes			0.47
			Sesquiterpene hydrocarbons			2.64
			Others			23.79
			Total (%)			99.99

P: peak; RT: retention time; RI: retention index; Cal: calculate; Lit: literature;

C0: The mean paw circumference before injection.

Ct: The mean paw circumference after carrageenan injection at a given time.

2.7. In-silico screening

After identifying the chemical constituents, in-silico simulation techniques such as ADME-Tox, *in-silico* predictions, and molecular docking simulations were employed to investigate the effects of all fourteen active molecules in AG-EO. During the initial stage, the pharmacokinetic properties of absorption, distribution, metabolism, excretion, and toxicity (ADMET) were predicted based on the five rules of Lipinski. Thereafter, the boiled egg of Egan and bioavailability radars were equally carried out to discover the desired physicochemical and pharmacokinetic profiles of the examined essential oil with the use of Pkcsm and Swissadme servers (Daina et al., 2017). In the second stage, molecular docking which has been applied previously for discovery and improvement of drugs (El fadili et al., 2022a), was applied to understand mechanisms of inhibition, antioxidant, antibacterial, and antifungal activities towards three targeted proteins encoded in protein data bank (PDB). Molecular docking was conducted by use of 2CDU.pdb, 2XCT.pdb, and 5TZ1.pdb, respectively (Bank, 2023). Initially, three-dimensional structures of proteins were converted from PDB format to PDBQT format, and then prepared by the addition of Gasteiger charges after the deletion of all water molecules (H_2O) and suspended co-crystallized ligands. Thereafter, the major compounds of essential oil were docked to the active sites of each prepared protein using Autodock-1.5.6 software (Morris et al., 2009). Finally, the intermolecular interactions of produced (protein–ligand) complexes were visualized using Discovery Studi-2021 software (BIOVIA Discovery Studio - BIOVIA - Dassault Systèmes®, 2023).

2.8. Statistical analysis

All experiments were executed by three independent tests (n = 3), and the obtained data were established as mean ± standard deviations (SD). Using GraphPad Prism 8.0 statistics software, the data analyses were performed. One-way analysis of variance (ANOVA) was used to compare the means, and a Tukey test was then performed. A statistically significant result was defined as a $p < 0.05$.

3. Results and discussion

3.1. Efficiency of microwave-assisted hydrodistillation (MHD)

Microwave assisted extraction is a valuable, green, novel technique applied in essential oil hydro-distillation (Selli et al., 2009). Due to its numerous benefits, including rapid and efficient transfer of energy and adequate heating, microwave-assisted hydro-distillation has been used in laboratories and industries (Zhang et al., 2011). Compared to other traditional extraction techniques, MHD exhibits excellent performance in increasing the quantity and quality of isolated oils, cutting down on costs and energy use, accelerating the extraction process, and reducing the amount of carbon dioxide released into the atmosphere (Jažo et al., 2022). The mechanism of action of microwave distillation is based on a defined power; the extraction yield increases with the extraction time. The dissolution of essential oil in water is facilitated by the interfacial area between the plant matrices and solvent, while the improvement in extraction efficiency with longer durations is attributed to the microwave adsorption energy. Microwave power serves as an engine to destroy the structure of cell membranes of plants, causing diffusion and dissolution of the oil in the solvent. The distillation temperature is elevated as a result of the amplified dielectric heating phenomena caused by higher microwave power. This increase in power also has a direct impact on the temperature. Consequently, a higher power level typically leads to an augmented yield and a faster extraction time (Mohamadi et al., 2013). The effectiveness of extraction through MHD is influenced by various factors, including extraction time, water/plant ratio, microwave power supply, and drying time, either individually or in combination (Moradi et al., 2018). Under the optimum conditions of an extraction duration of 20 min, microwave power of 600 W, a water-to-plant material ratio of 2 mL/g, and a drying period of seven days, the yield of AG-EO was found to be 4.17±0.041 % per 100 g of seeds. The volatile oil content of celery seed is approximately 2% (Zorga et al., 2020). The approach holds ecological significance as it reduces the need for the distillation stage, minimizes electricity usage, and saves time.

3.2. Phytochemical profile of AG-EO

Fourteen compounds, accounted for 99.99% of the total mass of AG-EO (Table 1, Fig. 1). AG-EO consisted primarily of limonene, which made up 64.58% of the total mass of AG-EO. Other compounds, present in smaller proportions included sedanenolide (15.38%), hexenyl salicylate (7.27%), naphthalene (6.30%), α-himachalene (1.88%), and β-pinene (1.53%). The chemical composition consisted mainly of monoterpene hydrocarbons, which accounted for 72.41% of the total. These results are consistent with those reported previously (Zorga et al., 2020) where the primary chemical constituents were limonene (76.9%), β-selinene (9.7%), sedanenolide (3.4%), 3-butylphtalide (3.6%), and α-selinene (1.4%). Similarly, Senegal *A. graveolens* collected from Senegal was abundant in limonene and β-selinene.

The chemical compositions of EOs exhibit variation and are influenced by numerous environmental factors. In the case of *A. graveolens* oils, these variations are contingent upon the following factors: plant part utilized, stage of the vegetative cycle, age of plants, the time of harvest, and genetic attributes (Barra, 2009). Essential oils are rich in phytoconstituents, including monoterpene hydrocarbons, oxygenated monoterpenoids, and sesquiterpene hydrocarbons sourced from various medicinal plants. These compounds are recognized for their substantial biological and pharmacological potential. Their documented capacities span the domains of antioxidation (Saini et al., 2021), antimicrobial activity (Bat-Özmatara, 2020), antiviral properties (Das et al., 2019),

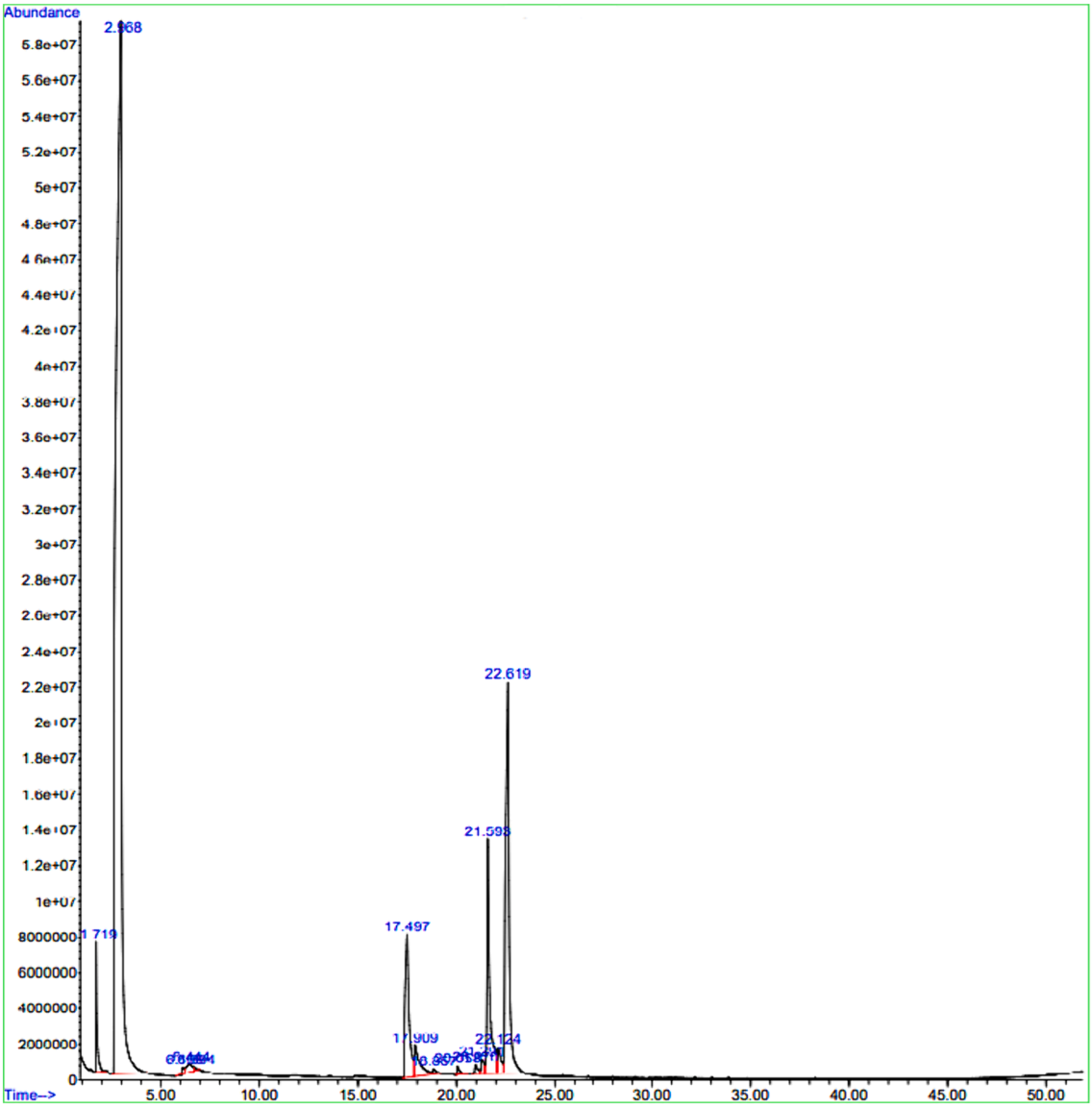

Fig. 1. GC-MS chromatogram of essential oil extracted from *Apium graveolens* seeds (AG-EO).

insecticidal efficacy (Kokotkiewicz and Luczkiewicz, 2016), and cytotoxic effects (Modaresi et al., 2012).

3.3. *In vitro antioxidant activity of AG-EO*

Antioxidant activity is a complicated process that usually occurs through several mechanisms (de Menezes et al., 2021). Due to its complexity, the antioxidant activity of pure compounds or extracts should be evaluated by more than a single test method. In this work, three classical antioxidant tests, namely DPPH, ABTS, and RP, were carried out together with total antioxidant capacity (TAC); tests and results were summarized (Fig. 2). The DPPH test revealed that AG-EO had significant antioxidant activity of 81 % of inhibition compared with 95 % for BHT standards (Fig. 2 a-b). This resulted in an IC_{50} value of 8.49 ± 0.00 µg/mL against 24.13 ± 0.00 µg for positive control (BHT) (Fig. 2c). This is consistent with the rsults of another study that found the antioxidant activity of AG-EO mixed with linalyl acetate and geranyl had significant scavenging of free radicals with DPPH assay (IC_{50} = 20.17 µL/mL) (Das et al., 2019). The antioxidant activity in the seeds of *A.graveolens* from Saudi Arabia exhibited a wide range of results, varying from 1.58 % ± 0.21 % to 32.45 % ± 0.2 % across different concentrations, which spanned from 0.25 to 5 mg/mL (Foudah et al., 2022). A previous study found that concentations of EO between 2.5 and 100 g/L quenched the stable free radical DPPH in a range between 34 and 52 % (Zorga et al., 2020). The IC_{50} value for AG-EO in the ABTS%$^{+}$ assay was moderate (5.09 ± 0.04 µg/mL) compared to synthetic standard antioxidant BHT (Fig. 2d). The AG-EO exhibited significantly greater antioxidant activity than those reported previously of IC_{50} = 9.56 µL/mL (Das et al., 2019). Alternatively, when the RP assay was used to evaluate the ability of the EO to transform ferric iron Fe^{3+} to ferrous iron Fe^{2+} (Thaipong et al., 2006), the antioxidant activity was found to be EC_{50} = 3.42 ± 0.01 µg/mL compared to ascorbic acid as standard (10.24 ± 0.05 µg/mL). Results of another study revealed that the range of absorption in ferric chloride increased from 0.043 ± 0.01 to 0.279 ± 0.02 as the concentration increased from 0.25 mg/mL to 5 mg/mL (Foudah et al., 2022). When the ammonium phosphomolybdate assay was carried out to determine the total antioxidant capacity of AG-EO. A total antioxidant capacity value of 245.93 ± 0.04 mg AAE/mL of Eo was observed compared with 257.26 ± 0.03 mg EAA/g for quercetin and 269.2 ± 0.12 mg EAA/g BHT as standards (Fig. 2e). In another study that assessed the essential antioxidant compounds in celery leaves, it was found that the total antioxidant capacity ranged from 41 % to 57 %

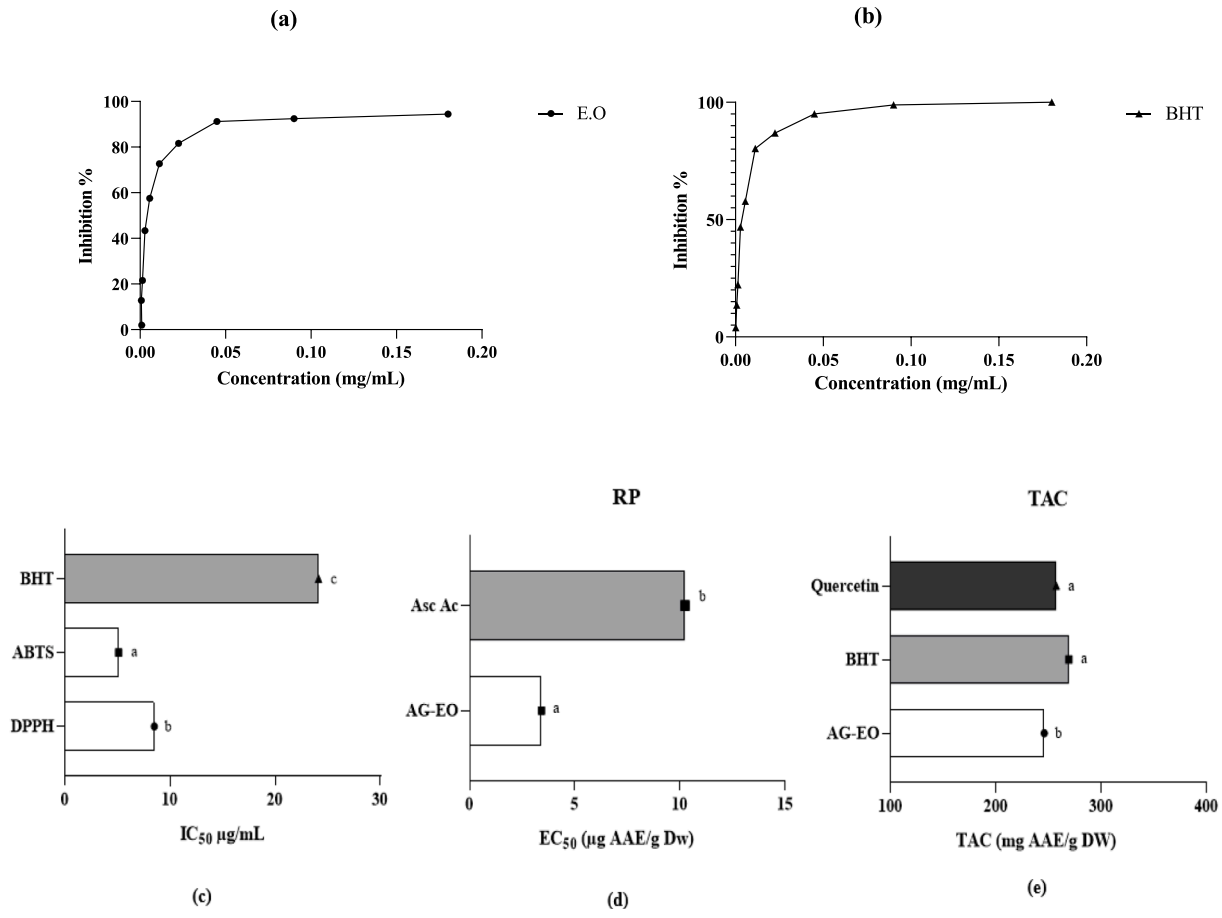

Fig. 2. Antioxidant activity of AG-EO using the DPPH and ABTS assays, Reducing power and total antioxidant capacity. The difference between bars with the same letters is not significant ($p < 0.05$).

Table 2
Disc diffusion test for essential oil from *A. graveolens*, performed on four pathogenic strains and using antibiotics for comparison. Inhibition zone diameter in mm. Results are expressed as mean ± SD.

Microbial strains	Inhibition zone diameter (mm)			
	Staphylococcus aureus	*Proteus mirabilis*	*Bacillus subtilis*	*Candida albicans*
AG-EO	35.00 ± 1.00	17.00 ± 1.50	19.00 ± 1.00	27.00 ± 0.41
Oxacilline	18.00 ± 0.00	0.00 ± 0.00	0.00 ± 0.00	–
Cefuroxime	0.00 ± 0.00	0.00 ± 0.00	0.00 ± 0.00	–
Fluconazole	–	–	–	13.00 ± 1.00
DMSO	6 ± 0.00	6 ± 0.00	6 ± 0.00	6 ± 0.00

Table 3
Minimum inhibitory concentrations (MIC) (mg/mL) of the EO extracted from *A. graveolens*.

Microbialstrains	Microdilution Method (MIC in mg/mL)			
	Staphylococcus aureus	*Proteus mirabilis*	*Bacillus subtilis*	*Candida albicans*
AG-EO	11.25 ± 1.00	0.71 ± 0.33	5.26 ± 2.65	3.75 ± 0.00
Oxacilline	0.312 ± 0.00	0.00 ± 0.00	0.00 ± 0.00	–
Fluconazole	–	–	–	7.50 ± 0.00

Table 4
Effect of AG-EO on carrageenan-induced paw oedema.

Diameter in cm					
Treatment	0 h	3 h	4 h	5 h	6 h
NaCl 0.9 %	2.6 ± 0.1	3.5 ± 0.0^{a}	3.5 ± 0.1^{a}	3.4 ± 0.0^{a}	3.45 ± 0.05^{a}
Indomethacin	2.35 ± 0.15	3.4 ± 0.00^{a}	3.45 ± 0.05^{a}	3.05 ± 0.05^{b}	2.75 ± 0.05^{b}
1.5 mL/kg	2.4 ± 0.2	3.45 ± 0.06^{a}	3.4 ± 0.2^{a}	3.15 ± 0.05^{b}	2.9 ± 0.0^{b}
5 mL/kg	2.42 ± 0.1	3.42 ± 0.0^{a}	3.1 ± 0.0^{ab}	2.9 ± 0.0^{b}	2.7 ± 0.0^{b}

Values of treated groups are expressed as diameter (cm) mean ± SD of 3 experiments. Values in the same column followed by the same letter are not significantly different by Tukey's multiple range test ($p < 0.05$).

in various celery leaf compounds at different levels of hydrolysis (Yildiz et al., 2008). By comparison, with the literature, the antioxidant activities of celery seed essential oil were described as weak or moderate. Numerous studies (Kokotkiewicz and Luczkiewicz, 2016; Glumac et al., 2023) have examined the antioxidant activity of EOs, most of which were carried out *in vitro* and *in vivo*. Antioxidants can have many effects, including scavenging free radicals, breaking down peroxides, and chelating metal ions (Saini et al., 2021). The compounds found in EOs, such as phenolic acids, terpenes, and sesquiterpenes, might be responsible for these activities. The precise mechanisms by which these compounds exert their antioxidant effects have not yet been fully explained. These compounds are known for their effects to scavenge free radicals and inhibit lipid oxidation (Tena et al., 2020). These substances operate as chain-breaking peroxyl-radical scavengers and display *in vitro* and *in*

Table 5
Prediction of the physicochemical properties of fourteen molecules identified in the extract from AG-EO.

Compounds number	Physico-chemical properties					Lipinski's five rules (No/Yes)
	MW	MR index	Log P	HBA	HBD	
Rule	≤500(g/mol)	130 ≥ MR index ≥ 40	<5	≤10	<5	
C 1	136.23	45.22	2.59	0	0	Yes
C 2	136.23	47.12	2.72	0	0	Yes
C 3	152.23	46.60	2.63	1	0	Yes
C 4	152.23	46.38	2.31	1	1	Yes
C 5	150.26	51.93	3.01	0	0	Yes
C 6	128.17	43.95	1.99	0	0	Yes
C 7	204.35	70.42	3.30	0	0	Yes
C 8	204.35	68.78	3.23	0	0	Yes
C 9	204.35	68.78	3.25	0	0	Yes
C10	204.35	68.78	3.31	0	0	Yes
C 11	224.38	70.89	3.14	1	1	Yes
C 12	220.26	63.31	3.08	3	1	Yes
C 13	133.15	38.97	2.02	2	0	Yes
C 14	192.25	55.91	2.69	2	0	Yes

vivo antioxidant action, which inhibits lipid peroxidation. Phenols also directly scavenge reactive oxygen species (Gülçin, 2012). Active substances in EOs of celery seeds are effective in adsorbing and neutralizing free radicals, quenching singlet, and triplet oxygen, or degrading peroxides, are the primary cause of their antioxidant activity (Amensour et al., 2009).

3.4. Antimicrobial activity of AG-EO

3.4.1. Determination of inhibition zone and minimum inhibitory concentration MIC

The antimicrobial activities of AG-EO were evaluated against a panel of four microorganisms using both qualitative and quantitative methods in the disk diffusion test. The presence or absence of inhibition zones, zone diameters, and MIC values were considered. AG-EO exhibited remarkable antimicrobial activities against all the microorganisms tested, indicating its effectiveness in inhibiting their growth (Tables 2 and 3). *Proteus mirabilis* exhibited significant potency as indicated by the MIC values discovered during the oil microwell dilution test. The maximum inhibition zones and MIC values for microbial strains sensitive to AG-EO were between 17 and 35 mm and 0.71 and 11.25 mg/ml, respectively. Overall, AG-EO displayed a more potent and extensive spectrum of antimicrobial activity. Gram-negative bacteria have an extra protective outer membrane that makes them much more resistant to antibacterial agents than their Gram-positive counterparts (Mayouf et al., 2019). In the disk diffusion test, AG-EO was most potent against the Gram-positive bacteria, *S. aureus and B. subtilis*. However, it also had a sizable inhibitory effect on yeast and Gram-negative bacteria, particularly the resilient bacterium, *Proteus mirabilis*. This finding is concurrent with results of other studies that AG-EO grown in Saudi Arabia exhibited superior antibacterial activity. The strongest antimicrobial activity was detected against Gram-positive bacteria and *Candida albicans* (Foudah et al., 2022).

β-pinene, limonene, and β-selinene were determined to be responsible for the biological activity of celery seeds oil. It has already been mentioned that EOs with greater limonene content, such as the essential oil of *Citrus aurantium dulcis, Citrus limonum* from Tahiti, or *Carum carvi* inhibited growth of *S. aureus* with MIC values of 16.5, 14.9 mg/mL, and 1.0 μL/mL, respectively (Everard et al., 1994). The yeast *C. albicans* was sensitive, and its growth was inhibited at a 3.75 mg/mL concentration. Limonene has destructive effects on the surface of yeast cells, thereby leading to apoptosis and strongly inhibiting the growth of *C. albicans* (Thakre et al., 2017). In addition, when tested against 12 different yeast strains, limonene (10 L) demonstrated more antifungal activity than the antibiotic Fungizone (50 μL) (Ünal et al., 2012). AG-EO has a potent antimicrobial effect against *E. coli,* and exhibits excellent activity against *P. aeruginosa, B. subtilis,* and *S. aureus* with MICs of 50 L/mL, 2 L/mL, 20 L/mL, and 30 L/mL, respectively (Dąbrowska et al., 2020) (Baananou et al., 2013; Din et al., 2015).

AG-EO exhibited substantial inhibition against aflatoxin-contaminated rice seeds, the most toxic strain of *Aspergillus flavus* (AFLHPR14), and fourteen other food-borne molds responsible for the deterioration of stored food commodities. The heightened effectiveness of the formulated treatment can be attributed to the synergistic interaction between the essential oil and its primary components (Valdiviesso-Ugarte et al., 2019). It was determined that the primary target of the formulation's antifungal activity was the fungal plasma membrane. This conclusion was supported by observations of reduced membrane ergosterol content, increased intracellular propidium iodide (PI)

Table 6
Prediction of the pharmacokinetic properties of fourteen molecules extracted from the essential oil of *Apium graveolens* (AG-EO).

Compounds Number	A	D		M							E	T		
	human intestinal Absorption	Blood-brain barrier permeability	Central nervous system permeability	Substrate		Inhibitor					Total Clearance	AMES test of toxicity	Hepatotoxicity	Skin Sensitization
				Cytochromes										
				2D-6	3A-4	1A-2	2C-19	2C-9	2D-6	3A-4				
	(% Absorbed)	(Log BB)	(Log PS)	(No/Yes)							Numeric (Log ml/min/kg)	(No/Yes)		
C 1	95.984	0.829	−1.867	No	No	No	No	No	No	No	0.03	No	No	No
C 2	95.898	0.725	−2.37	No	No	No	No	No	No	No	0.213	No	No	**Yes**
C 3	96.715	0.359	−2.736	No	No	No	No	No	No	No	1.159	No	No	**Yes**
C 4	94.798	0.739	−2.392	No	No	No	No	No	No	No	0.049	No	No	**Yes**
C 5	94.052	0.783	−2.215	No	No	No	No	No	No	No	1.516	No	No	No
C 6	94.878	0.437	−1.244	No	No	**Yes**	No	No	No	No	0.198	No	No	**Yes**
C 7	94.682	0.663	−2.555	No	No	No	No	No	No	No	1.291	No	No	**Yes**
C 8	95.429	0.722	−2.325	No	No	No	No	No	No	No	1.1	No	No	**Yes**
C 9	95.712	0.735	−2.169	No	No	No	No	**Yes**	No	No	1.088	No	No	**Yes**
C 10	96.439	0.821	−1.428	No	No	No	No	No	No	No	1.174	No	No	**Yes**
C11	93.501	0.64	−1.562	No	**Yes**	No	No	No	No	No	1.041	No	No	**Yes**
C12	90.973	0.297	−1.955	No	No	**Yes**	**Yes**	No	No	No	0.745	No	No	No
C 13	95.552	0.006	−1.974	No	No	**Yes**	No	No	No	No	0.844	No	No	**Yes**
C 14	96.202	0.589	−2.526	No	No	**Yes**	No	No	No	**Yes**	1.422	No	No	**Yes**

A: Absorption; D: Distribution; M: Metabolism; E: Excretion; T: Toxicity.

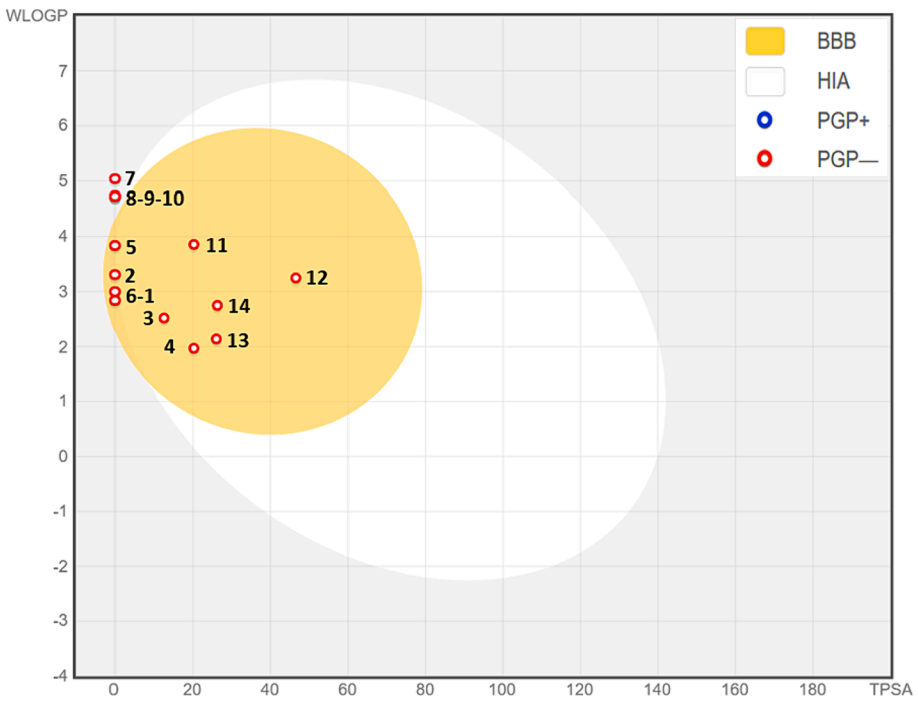

Fig. 3. Egan Boild-Egg model of the fourteen chemical compounds extracted from *Apium graveolens* essential oil.

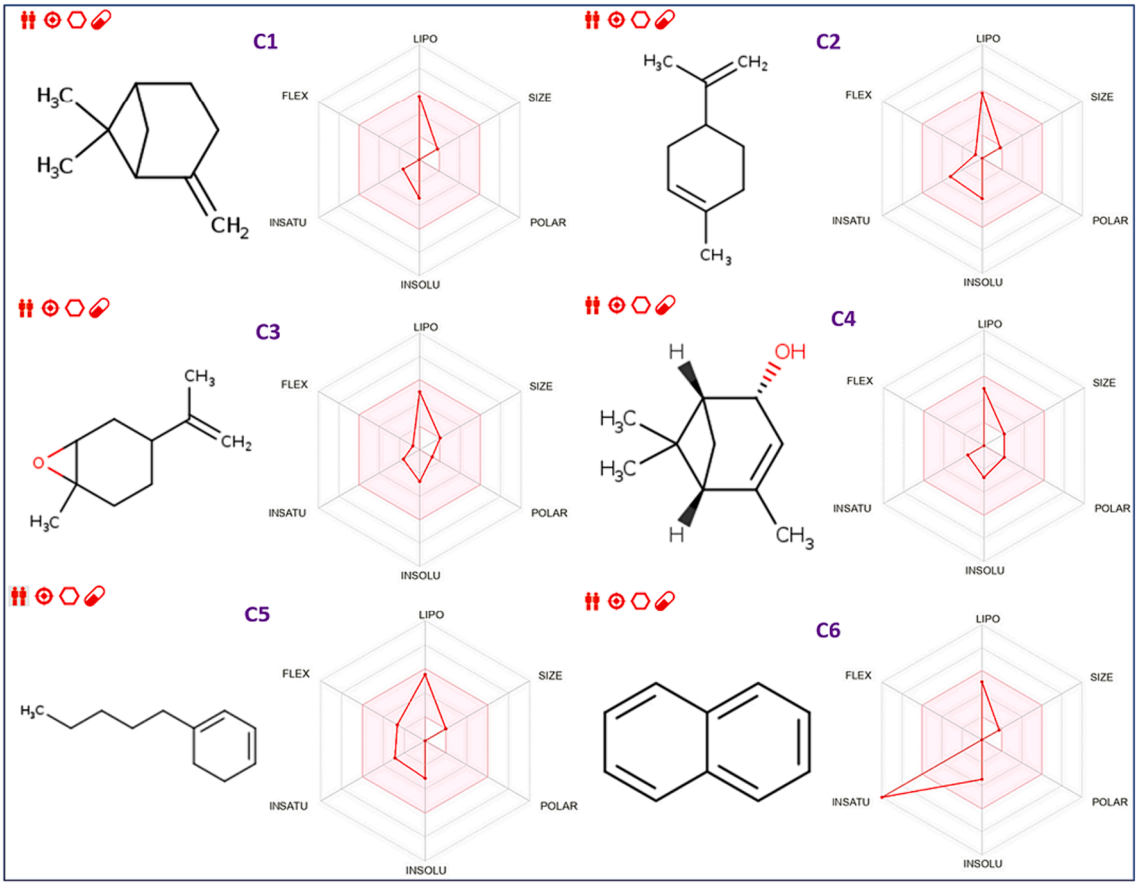

Fig. 4. Bioavailability radars of the fourteen chemical compounds extracted from AG-EO.

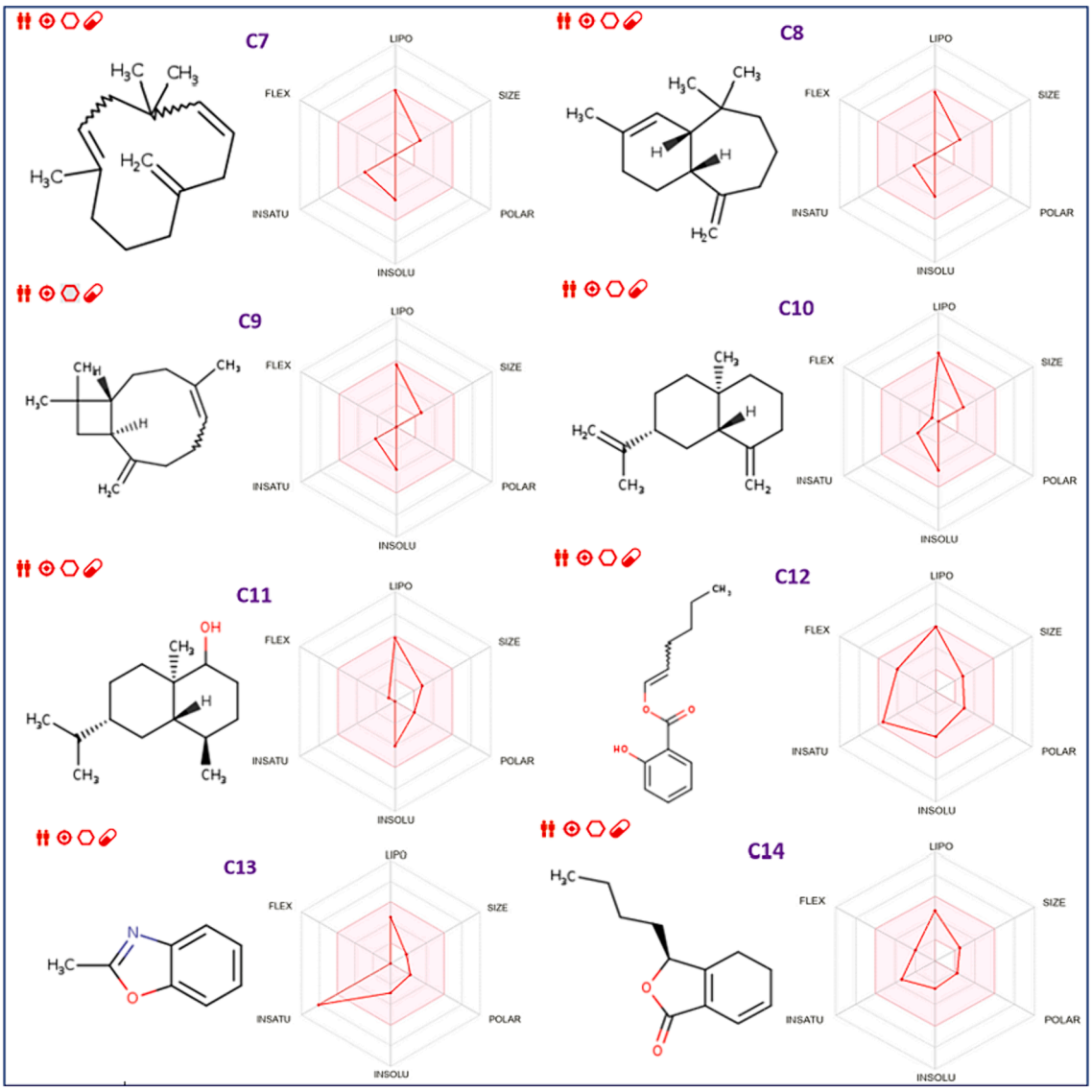

Fig. 4. (*continued*).

fluorescence, enhanced leakage of cellular ions (sodium, potassium, and calcium), and the absorption of materials within the 260–280 nm range (Dwivedy et al., 2016).

Various strains of bacteria exhibit differential sensitivities to EOs (El-Beltagi et al., 2020). It has been suggested that the primary mechanisms of action is irreparable damage to the bacterial cell wall and membrane (Thiam et al., 2020) which then disrupts enzymes, compromising the genetic material of bacteria, and evolving fatty acid hydroperoxides induced by oxygenation of unsaturated fatty acids (Rana et al., 2022). EOs can damage lipids and proteins and cause the cytoplasm to clot. They would function in the same way as additional phenolics. The ranges of cell coagulation, active transport, electron flow, and proton motive force alteration. Instead, lipid molecules connect enzymes like ATPases that are present in the cytoplasmic membrane (Kokotkiewicz and Luczkiewicz, 2016). Hydrophobicity of EOs and their constituents allows them to partition in the lipids of bacterial cell membranes and mitochondria, warping their structure and making them more susceptible to antimicrobial action, which results in leakage of cell contents (Nagella et al., 2012). Additionally, the chemical makeup of the individual essential oil components influences their specific manner of measurement and antibacterial activity (Ayman et al., 2008). Similarly, several studies have revealed how EOs can inhibit biofilm formation by inhibiting communication between bacterial cells (Sheikh et al., 2023). There is no discernible difference in biological activity when comparing celery seed essential oils obtained through conventional hydrodistillation to those obtained through microwave-assisted distillation (Majda et al., 2020).

3.5. Carrageenan-induced rat paw test

The anti-inflammatory effect of AG-EO was assessed using the carrageenan-induced rat paw test. The circumference/diameter of the rat's paw (n = 5) and the percentage of the paw volume (cm) at 3, 4, 5, and 6 h post-carrageenan (1 %) injection are presented in the Table 4. The data indicate an increase in paw volume over time, with maximum swelling observed at 3 h post-injection for all extracts. At 4 h post-injection, the vehicle (NaCl (0.9 %)) exhibited the highest circumference (3.5 ± 0.1 cm). Conversely, the groups treated with AG-EO (1.5 mL/kg) (3.4 ± 0.2 cm), AG-EO (5 mL/kg) (3.1 ± 0.0 cm), and Indomethacin® (3.45 ± 0.05 cm) displayed reduced circumference, indicative of an anti-inflammatory effect. Notably, the AG-EO (5 mL/kg) group exhibited the highest inhibition of edema at peak inflammation. After 6 h, both AG-EO extracts showed significant reductions in paw size compared to the control group at $p < 0.05$.

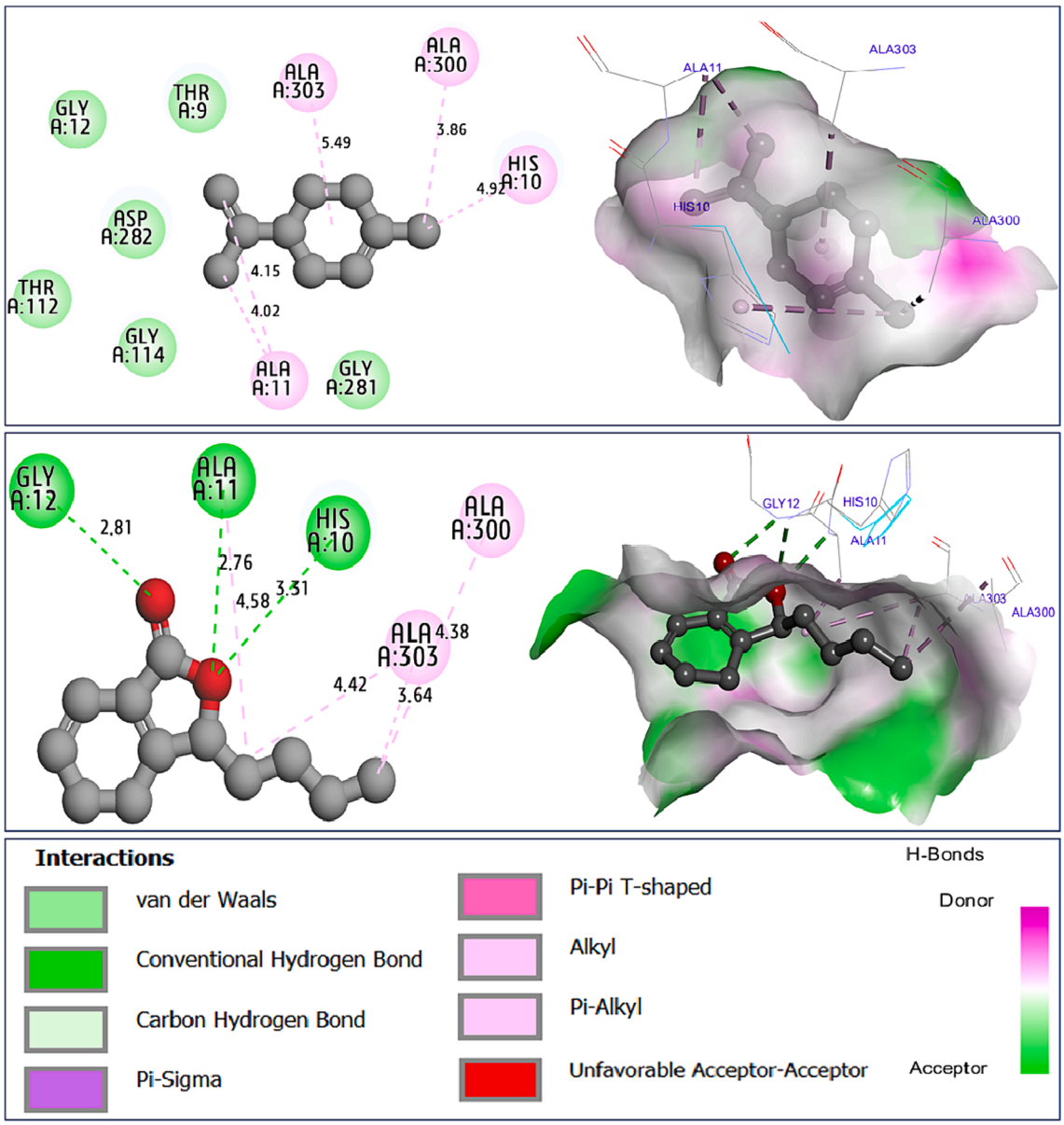

Fig. 5. Intermolecular interactions in two and three dimensions, resulted between limonene (C2) and sedanenolide (C14) towards NADPH oxidase protein from *Lactobacillus sanfranciscensis* (2CDU.pdb).

The carrageenan-induced paw edema protocol is a well-established model for investigating the anti-inflammatory effects of natural products *in vivo*. Carrageenan injection induces early hyperemia, triggering the release of mediators such as bradykinin, histamine, and serotonin, followed by a second phase characterized by prostaglandin release and leukocyte migration (Agour et al., 2022).

AG-EO demonstrated anti-inflammatory effects, with confirmed inhibitory effects on lipid mediators such as phospholipase A2 and cyclooxygenase. Additionally, its catalytic effects on cyclooxygenase and prostaglandin biosynthesis were validated. Phenolic acids and flavonoids play pivotal roles in the anti-inflammatory processes of both plants, with the hydroxyl group of flavonoids reported to influence oral anti-inflammatory activity (Mssillou et al., 2022).

3.6. ADME and prediction of toxic potency of AG-EO

Based on Lipinski's five rules, which require chemical compounds to meet the following conditions in order to have pharmaceutical properties similar to approved drugs: molecular weight (MW) does not exceed 500 g/mol, the index of molar refractivity (MR index) included in [40, 130] rang, lipophilicity in octanol/water solvent defined by a LogP less than five, Acceptors and donors of Hydrogen bonds (HBA and HBD) must be inferior than ten and five, successively (Lipinski, 2004). In this respect, we note that all the compounds satisfy the critical thresholds for physicochemical properties as stipulated by Lipinski (Table 5).

In addition, the prediction of pharmacokinetic features of ADMET (El fadili et al., 2022b; Jia et al., 2020) show that the compounds under investigation were well absorbed, as the results for human intestinal absorption exceeded 90 %. Also, the blood–brain barrier and central nervous system permeabilities were included in [0, 1] Log BB and [-1, −2] Log PS, respectively. The metabolism analysis indicated that the compound labeled C11 was predicted as a substrate of 3A4 cytochrome, while the compounds labeled C6, C12, C13, and C14 were predicted as potent inhibitors of 1A2 cytochrome. Then, C9, C12, and C14 were predicted to be inhibitors of 2C9, 2C19, and 3A4 cytochromes, respectively. Fortunately, results of the AMES mutagenicity test confirmed that all molecules in AG-EO were predicted to not be mutagenic and do not cause hepatotoxicity. However, the majority of the constituents were

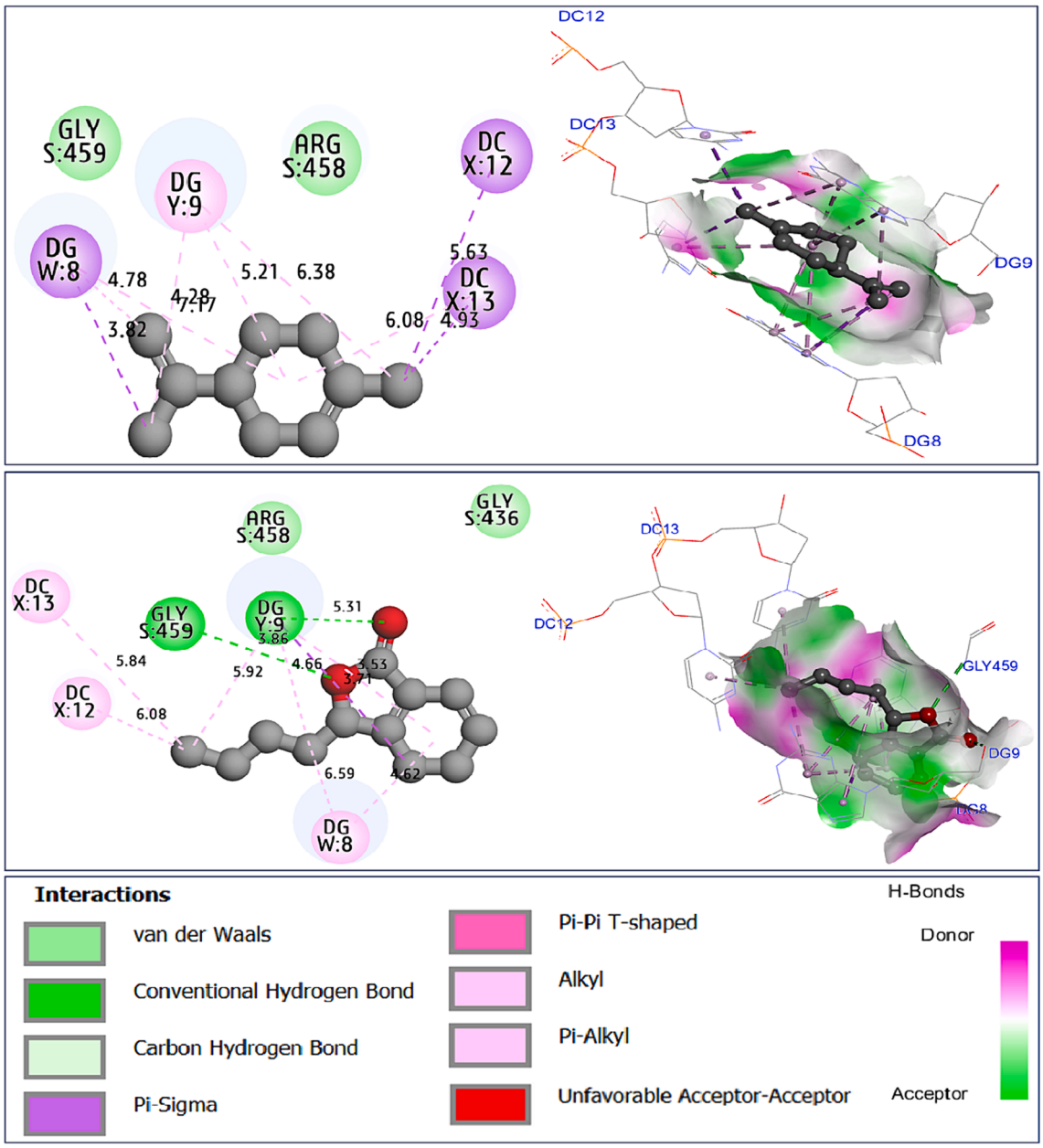

Fig. 6. Intermolecular interactions in two and three dimensions, resulted between limonene (C2) and sedanenolide (C14) towards antibiotic protein from *Staphylococcus aureus* (2XCT.pdb).

predicted to cause skin allergies, except for molecules labeled as C1, C5, and C12, which have been shown to be free of undesirable effects (Table 6).

Results of the predictive model of the Egan Boiled-Egg (Fig. 3), confirms that all extracted molecules from AG-EO are part of Boiled-egg yolk, so they are predicted to passively permeate through the blood–-brain barrier, except for four chemical compounds, C7, C8, C9, and C10 which weren't part of egg yol. Also, the compounds were located as red dots, so they were predicted not to be effluated from the central nervous system by the P-glycoprotein (Daina and Zoete 2016).

Based on six physicochemical characteristics, included in the bioavailability, radars test, which include lipophilicity, flexibility, unsaturation, solubility, size, and polarity (Fig. 4) it can be concluded that all examined molecules are part of the ideal area of bioavailability radars as colored in pink, except for C6, and C13, due to their inappropriate unsaturation. Therefore, the majority of molecules show great oral bioavailability (El fadili et al., 2023b,c).

3.7. Molecular docking

To explore their inhibition mechanisms towards antioxidant, antibacterial, and antifungal activities, six molecular docking simulations were conducted for two major compounds, namely: limonene (C2) and sedanenolide (C14), which represented 64.58, and 15.38 % of the mass of AG-EO, respectively, on three targeted proteins deemed to be important in determining the observed effects in line with their biological functions against pathogenic strains.

Results of docking simulations demonstrate that limonene (C2) and sedanenolide (C14) were docked to the active sites of NADPH oxidase protein from *Lactobacillus sanfranciscensis* (**2CDU**.pdb), with lowest binding energies of −**5.32** and −**5.76** in Kcal/mol, and sharing a variety of common chemical bonds with those that bind to His10, Ala11, Ala300, and Ala303 amino acids residues (AARs), more than one additional Hydrogen bond, best recognized for its stabilizing effect on the produced (ligand–protein) complex, which was detected between Gly12

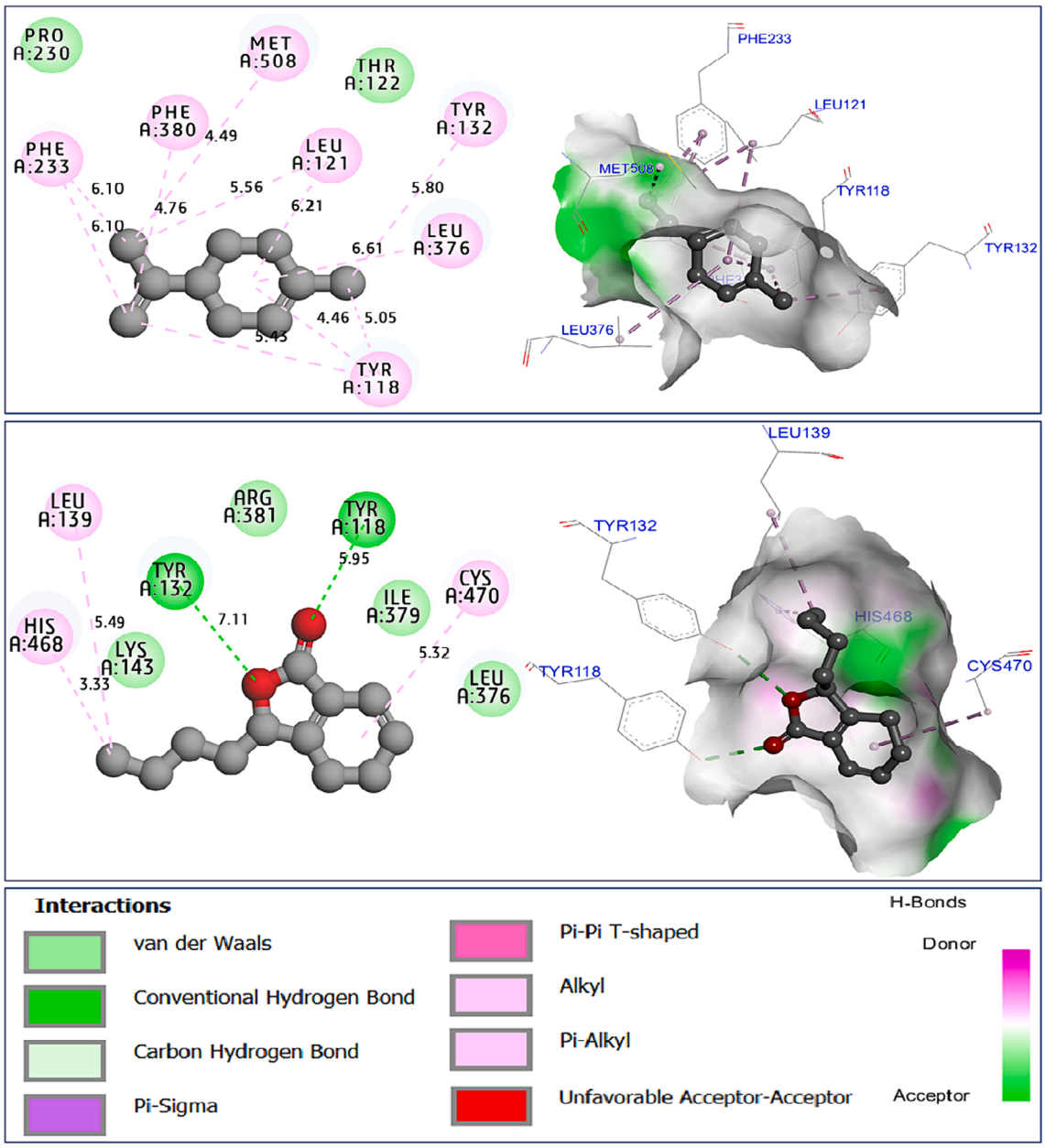

Fig. 7. Intermolecular interactions in two and three dimensions, resulted between limonene (C2) and sedanenolide (C14) towards CYP51 protein from *Candida albicans* (5TZ1.pdb).

AAR in A chain and the compound labeled C14, namely sedanenolide, as displayed in Fig. 5.

The same candidate ligands were equally docked to the active sites of antibiotic protein from *Staphylococcus aureus* (encoded by **2XCT**.pdb), with binding energies of **−5.22**, and **−6.71** in Kcal/mol, indicating similar intermolecular interactions like those produced towards DC12, and DC13 AARs in the X chain, more than DG9 AAR in the Y chain, in addition to another common bond which was created with DG8 in the W chain, as well as one Hydrogen bond type resulted from the Gly459 AAR in the S chain, in complex with the sedanenolide compound (C14), as pictured in Fig. 6.

To explore possible mechanisms of antifungal activity of AG-EO, the leading C2, and C14 compounds were subjected to molecular docking with the crystal structure of sterol 14-alpha demethylase (CYP51) from *Candida albicans* in complex with the tetrazole-based antifungal drug candidate VT1161 encoded in protein data bank (PDB) by **5TZ1**.pdb, with binding energies of **−6.75** Kcal/mol, and **−6.98** Kcal/mol, respectively. Limonene molecule labeled C2 produced a variety of chemical bonds, including seven alkyl bonds, which were detected towards Tyr118, Tyr132, Leu121, Leu376, Phe233, Phe388, and Met508 AARs in A chain. While the sedanenolide compound, labeled C14 created two Hydrogen bonds with Tyr118 and Tyr132 AARs, in addition to three Alkyl bonds formed with His468, Leu139, and Cys470 AARs in the A chain of the same receptor protein (Fig. 7).

The processes of molecular docking were successfully validated since the major compounds (C2 and C14) were actually docked to the active sites of each targeted protein, in complex with their co-crystallized ligands (El fadili et al., 2023a), in a manner that is similar intermolecular interactions with NADPH oxidase, antibiotic, and CYP51 proteins. Where Ala11, Ala300, Asp282, Lys134, Ser115, Thr9, Glu32, Val81, and Met33 AARs in A chain, and Phe425 AAR in B chain: are the active sites of NADPH oxidase protein (2CDU), While Da13 AAR in Y chain, DG9 AAR in X chain, Ser1084 AAR in S chain, and MN2001 AAR in W chain: are the active sites of 2XCT.pdb protein, so that Arg381, Lys143, Tyr118,

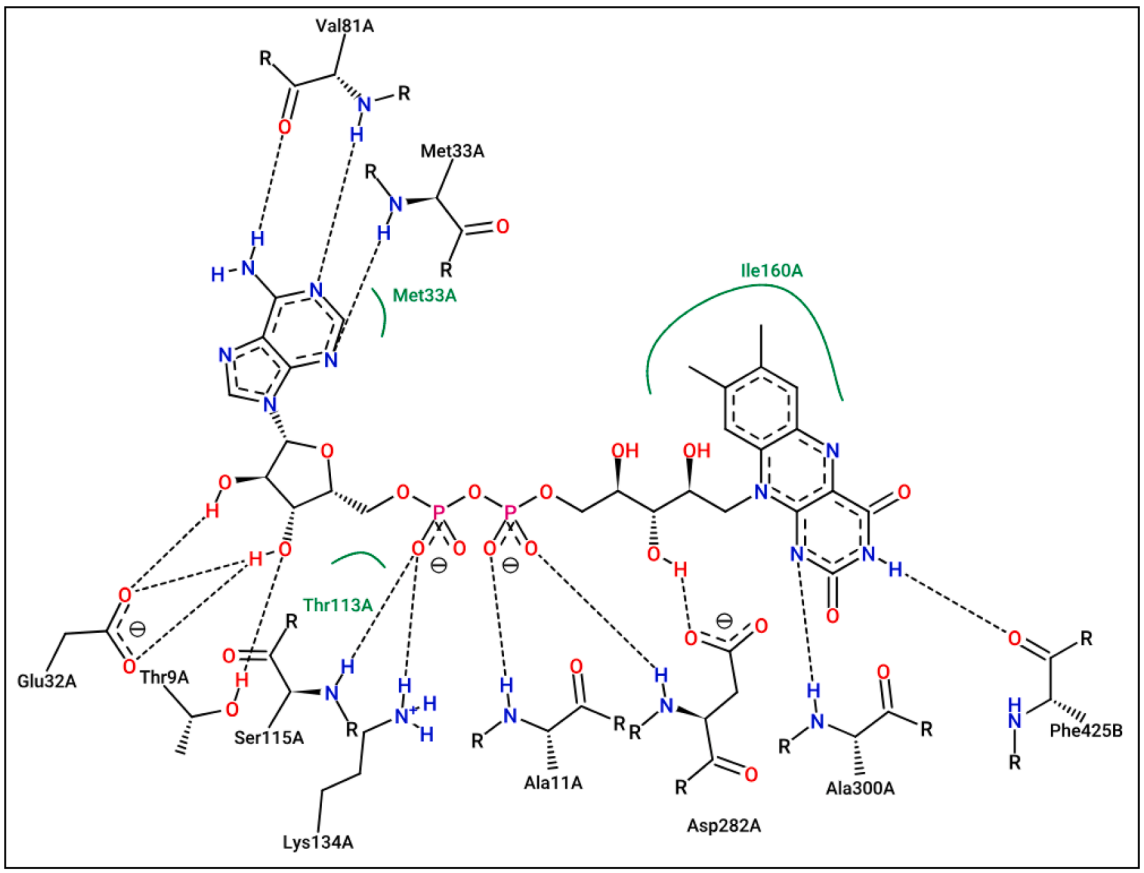

❖ **Active sites of 2CDU.pdb protein**

Fig. 8. Active sites of antioxidant (2CDU.pdb), antibacterial (2XCT.pdb), and antifungal (5TZ1.pdb) proteins towards Flavin-adenine dinucleotide (**Above**), Ciprofloxacin (**Left**), and Tetrazole-based antifungal drug candidate VT1161 (**Right**), respectively.

Tyr132, His468, and Fe601 AARs in A chain: are the active sites of 5TZ1. pdb protein (Fig. 8).

Based on the results of these molecular simulations processes, it was concluded that antioxidant activity of AG-EO is likely occurred due to creation of the chemical bonds detected towards **His10, Ala11, Ala300, and Ala303** AARs. So that antibacterial activity of AG-EO is explained by production of **DG8, DG9, DC12, and DC13** AARs. Finally, the antifungal activity of the essential oil is well explained by the detection of **Tyr118, and Tyr132** AARs. Additionally, the obtained values of binding energies in Kcal/mol are largely negative and do not exceed the −5.000 Kcal/mol threshold, so they indicate good levels of molecular stability in energetic order (Gu et al., 2024).

These results are consistent with results recently published (Sama-ae et al., 2023), which demonstrated biological activity of antifungal molecules from natural sources towards Lanosterol 14-alpha demethylase (CYP51). This indicates several similar intermolecular interactions, including the active sites of CYP51 protein from *Candida albicans*. In another study (Jeddi et al., 2023), that examined the antioxidant effects of two major compounds in EO extracted from the *Lavandula angustifolia* Mill., towards NADPH oxidase protein. In fact, the major compounds of the plant under study, were similarly docked to the active sites of responsible protein, sharing broadly equivalent intermolecular interactions. Similar intermolecular interactions were observed for binding of N-substituted 1-cyclopropyl-6,7-difluoro-8-methoxy-4-oxo-1,4-dihydroquinoline-3-carbohydrazide derivatives, which have been synthesized. These synthetic compounds towards the same targeted protein encoded by 2XCT and were correlated with antibacterial activity against *Staphylococcus Aureus, Micrococcus Luteus, Bacillus subtilis* and the pathogens Gram-negative *Escherichia Coli, Pseudomonas aeruginosa* and *Flavobacterium Devorans*.pdb, as authored by Munshi et al (Munshi et al., 2023).

3.8. Research limitations

This investigation into the antimicrobial, antioxidant, and anti-inflammatory properties of *Apium graveolens* essential oil offers a compelling rationale for further clinical studies. However, it would be beneficial to conduct *in vitro* testing of individual compounds present in this oil to precisely elucidate their efficacy. Additionally, while this study provides valuable insights into the antimicrobial and antioxidant activities of AG-EO, it lacks a detailed exploration of the molecular mechanisms underlying these effects.

The *in-silico* simulation suggests the safety of the chemical constituents found in AG-EO. Nonetheless, to comprehensively assess the toxicity profile of this essential oil, further investigations utilizing animal models are warranted. These studies should evaluate the potential toxicity of AG-EO over extended periods of time to ensure a thorough understanding of its safety profile.

4. Conclusions

Essential oil derived from *A. graveolens* (AG-EO) is abundant in monoterpenes and sesquiterpenes, including compounds like limonene, hexenyl salicylate, β-pinene, sedanenolide, and naphthalene, among others. The utilization of PASS prediction in online theoretical studies has indicated moderate antioxidant, antifungal, and antibacterial

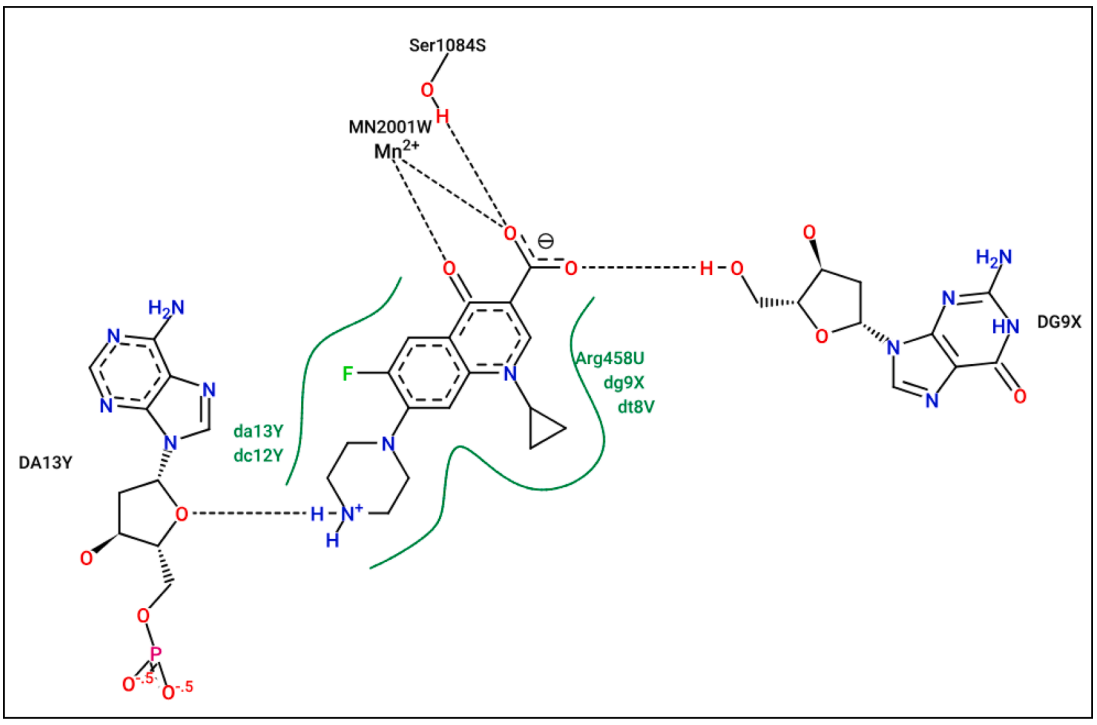

❖ **Active sites of 2XCT.pdb protein**

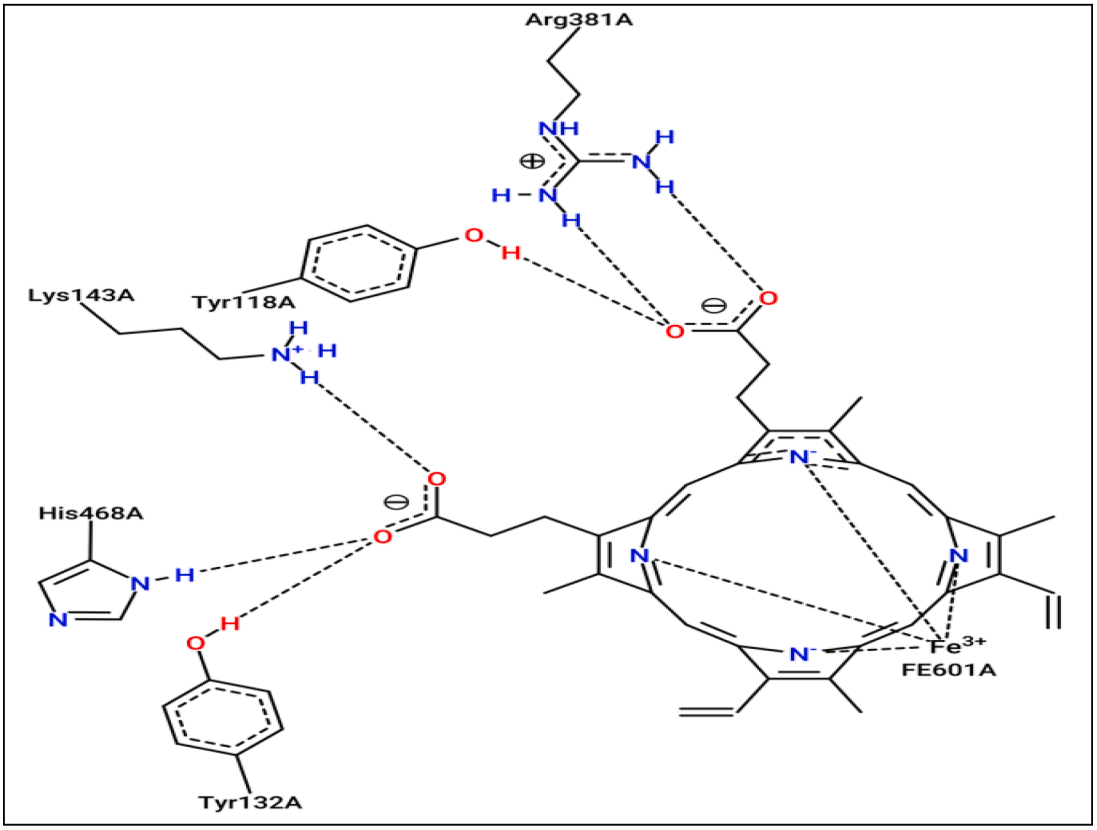

❖ **Active sites of 5TZ1.pdb protein**

Fig. 8. (*continued*).

properties for AG-EO. Furthermore, *in-silico* analyses have revealed that AG-EO exhibits drug-like properties, complying with Lipinski's rule of five, with good ADMET profiles, displaying greater absorption, while exerting minimal influence on CYP enzymes. The predictive toxicological assessments of this essential oil have suggested its safety and suitability for biological applications and its potential as a medicinal agent.

The mechanisms for inhibition of biological activities for major compounds were investigated by use of molecular docking simulations, and effectively validated towards the active sites of responsible proteins. The potential of AG-EO is highlighted by its potent antibacterial effects against gram-positive strains such as *Staphylococcus aureus* and *Bacillus subtilis*, along with substantial antifungal activity against *Candida albicans*. AG-EO has also exhibited remarkable antioxidant activity, as confirmed by DPPH, ABTS, RP, and TAC assays. Furthermore, the anti-inflammatory activity of AG-EO underscores its excellent efficacy. Therefore, it can be reasonably inferred that the AG-EO examined in this study presents a promising prospect as a natural source of antioxidants and preservatives for application in food and therapeutic products.

Funding

This research was funded by the Researchers Supporting Project (No. RSPD2024R816), King Saud University, Riyadh, Saudi Arabia.

CRediT authorship contribution statement

GN, MEF, BL, ElD: Conceptualization, writing – original draft, supervision, project administration. **LZ, SM, OZ, MD, IM:** Conceptualization, writing – review & editing, validation, formal analysis. **MAMA-S:** Writing- reviewing & editing, validation, resources. **HKG:** Funding acquisition, visualization, writing- reviewing & editing. **JPG:** Writing-reviewing & editing. **BL, ElD:** supervision.

Acknowledgments

The authors extend their appreciation to Researchers Supporting Project (No. (RSPD2024R816), King Saud University, Riyadh, Saudi Arabia.

References

Agour, A., Mssillou, I., Es-safi, I., Conte, R., Mechchate, H., Slighoua, M., Amrati, F.-Z., Parvez, M.K., Numan, O., Bari, A., Lyoussi, B., Derwich, E., 2022. The Antioxidant, Analgesic, Anti-Inflammatory, and Wound Healing Activities of Haplophyllum Tuberculatum (Forsskal) A. Juss Aqueous and Ethanolic Extract. Life 12 (10), 1553. https://doi.org/10.3390/life12101553.

Amensour, M., Sendra, E., Abrini, J., Pérez-Alvarez, J.A., Fernández-López, J., 2009. Total phenolic content and antioxidant activity of myrtle (Myrtus communis) extracts. Nat. Prod. Commun. juin, 819–824.

Anon. s. d. BIOVIA Discovery Studio - BIOVIA - Dassault Systèmes® . Consulté 22 octobre 2023 (https://www.3ds.com/products-services/biovia/products/molecular-modeling-simulation/biovia-discovery-studio/).

Ayman E.M., Nadia, M., Abd El-Motaleb, et Nadia H. Assem, 2008. Food Technology Research Institute, Agricultural Research Center, Giza, Egypt. Arab Universities Journal of Agricultural Sciences 16(1):115-25. doi: 10.21608/ajs.2008.14615.

Baananou, S., Bouftira, I., Mahmoud, A., Boukef, K., Marongiu, B., Boughattas, N.A., 2013. Antiulcerogenic and Antibacterial Activities of *Apium Graveolens* Essential Oil and Extract. Nat. Prod. Res. 27 (12), 1075–1083. https://doi.org/10.1080/14786419.2012.717284.

Balouiri, M., Sadiki, M., Ibnsouda, S.K., 2016. Methods for in vitro evaluating antimicrobial activity: a review. J. Pharm. Anal. 6 (2), 71–79. https://doi.org/10.1016/j.jpha.2015.11.005.

Bank, RCSB Protein Data. s. d. RCSB PDB: Homepage . Consulté 22 octobre 2023 (https://www.rcsb.org/).

Barra, A., 2009. Factors affecting chemical variability of essential oils: a review of recent developments. Nat. Prod. Commun. 4 https://doi.org/10.1177/1934578X0900400827.

Bat-Özmatara, Merve. 2020. THE ANTIOXIDANT ACTIVITY OF APIUM GRAVEOLENS . (1).

Ben Abada, M., Haouel Hamdi, S., Masseoud, C., Jroud, H., Bousshih, E., Mediouni Ben Jemâa, J., 2020. Variations in chemotypes patterns of tunisian rosmarinus officinalis essential oils and applications for controlling the date moth ectomyelois ceratoniae (Pyralidae). S. Afr. J. Bot. 128, 18–27. https://doi.org/10.1016/j.sajb.2019.10.010.

Dąbrowska, J.A., Kunicka-Styczyńska, A., Śmigielski, K.B., 2020. Biological, chemical, and aroma profiles of essential oil from waste celery seeds (*Apium Graveolens* L.). J. Essent. Oil Res. 32 (4), 308–315. https://doi.org/10.1080/10412905.2020.1754937.

Daina, A., Michielin, O., Zoete, V., 2017. SwissADME: a free web tool to evaluate pharmacokinetics, drug-likeness and medicinal chemistry friendliness of small molecules. Sci. Rep. 7 (1), 42717. https://doi.org/10.1038/srep42717.

Daina, A., Zoete, V., 2016. A BOILED-egg to predict gastrointestinal absorption and brain penetration of small molecules. ChemMedChem 11 (11), 1117–1121. https://doi.org/10.1002/cmdc.201600182.

Das, Somenath, Vipin Kumar Singh, Abhishek Kumar Dwivedy, Anand Kumar Chaudhari, Neha Upadhyay, Akanksha Singh, Deepika, et Nawal Kishore Dubey. 2019. Antimicrobial Activity, Antiaflatoxigenic Potential and in Situ Efficacy of Novel Formulation Comprising of Apium Graveolens Essential Oil and Its Major Component. *Pesticide Biochemistry and Physiology* 160:102-11. doi: 10.1016/j.pestbp.2019.07.013.

de Menezes, B., Brummelhaus, L.M., Frescura, R.D., Villetti, M.A., Barcellos, M., 2021. A critical examination of the DPPH Method: mistakes and inconsistencies in stoichiometry and IC50 determination by UV–Vis Spectroscopy. Anal. Chim. Acta 1157, 338398. https://doi.org/10.1016/j.aca.2021.338398.

Din, Zakir Ud, Anwar Ali Shad, Jehan Bakht, Inam Ullah, et Saleem Jan. 2015. In Vitro Antimicrobial, Antioxidant Activity and Phytochemical Screening of Apium Graveolens. *Pak. J. Pharm. Sci.*.

Dwivedy, A.K., Kumar, M., Upadhyay, N., Prakash, B., Dubey, N.K., 2016. Plant essential oils against food borne fungi and mycotoxins. Curr. Opin. Food Sci. 11, 16–21. https://doi.org/10.1016/j.cofs.2016.08.010.

El fadili, Mohamed, Mohammed Er-rajy, Hamada Imtara, Mohammed Kara, Sara Zarougui, Najla Altwaijry, Omkulthom Al kamaly, Aisha Al Sfouk, et Menana Elhallaoui. 2022. 3D-QSAR, ADME-Tox In Silico Prediction and Molecular Docking Studies for Modeling the Analgesic Activity against Neuropathic Pain of Novel NR2B-Selective NMDA Receptor Antagonists. Processes 10(8):1462. doi: 10.3390/pr10081462.

El fadili, Mohamed, Mohammed Er-Rajy, Mohammed Kara, Amine Assouguem, Assia Belhassan, Amal Alotaibi, Nidal Naceiri Mrabti, Hafize Fidan, Riaz Ullah, Sezai Ercisli, Sara Zarougui, et Menana Elhallaoui. 2022. QSAR, ADMET In Silico Pharmacokinetics, Molecular Docking and Molecular Dynamics Studies of Novel Bicyclo (Aryl Methyl) Benzamides as Potent GlyT1 Inhibitors for the Treatment of Schizophrenia. *Pharmaceuticals* 15(6):670. doi: 10.3390/ph15060670.

El fadili, Mohamed, Mohammed Er-rajy, Wafa Ali Eltayb, Mohammed Kara, Amine Assouguem, Asmaa Saleh, Omkulthom Al Kamaly, Sara Zerougui, et Menana Elhallaoui. 2023. In-Silico Screening Based on Molecular Simulations of 3,4-Disubstituted Pyrrolidine Sulfonamides as Selective and Competitive GlyT1 Inhibitors . Arab. J. Chem. 105105. doi: 10.1016/j.arabjc.2023.105105.

El fadili, Mohamed, Mohammed Er-rajy, Wafa Ali Eltayb, Mohammed Kara, Hamada Imtara, Sara Zarougui, Nawal Al-Hoshani, Abdullah Hamadi, et Menana Elhallaoui. 2023. An In-Silico Investigation Based on Molecular Simulations of Novel and Potential Brain-Penetrant GluN2B NMDA Receptor Antagonists as Anti-Stroke Therapeutic Agents. J. Biomol. Struct. Dyn. 1-15. doi: 10.1080/07391102.2023.2232024.

El fadili, Mohamed, Mohammed Er-rajy, Hamada Imtara, Omar M. Noman, Ramzi A. Mothana, Sheaf Abdullah, Sara Zerougui, et Menana Elhallaoui. 2023. QSAR, ADME-Tox, Molecular Docking and Molecular Dynamics Simulations of Novel Selective Glycine Transporter Type 1 Inhibitors with Memory Enhancing Properties. *Heliyon* 9 (2):e13706. doi: 10.1016/j.heliyon.2023.e13706.

El-Beltagi, H.S., Dhawi, F., Aly, A.A., El-Ansary, A.E., 2020. Chemical compositions and biological activities of the essential oils from gamma irradiated celery (Apium Graveolens L.). Seeds. Notulae Botanicae Horti Agrobotanici Cluj-Napoca 48 (4), 2114–2133. https://doi.org/10.15835/nbha48412115.

Everard, JohnD, Riccardo Cucci, Susan C. Kann, JamesA Flore, et Wayne H. Loescher. 1994. Gas Exchange and Carbon Partitioning in the Leaves of Celery (Apium Graveolens 1.) at Various Levels of Root Zone Salinity' .

Foudah, A.I., Alqarni, M.H., Alam, A., Salkini, M.A., Ross, S.A., Yusufoglu, H.S., 2022. Phytochemical screening, in vitro and in silico studies of volatile compounds from petroselinum crispum (mill) leaves grown in saudi arabia. Molecules 27 (3), 934. https://doi.org/10.3390/molecules27030934.

Glumac, M., Jažo, Z., Paštar, V., Golemac, A., Čulić, V.Č., Bektić, S., Radan, M., Carev, I., 2023. Chemical profiling and bioactivity assessment of helichrysum italicum (Roth) G. Don. Essential Oil: Exploring Pure Compounds and Synergistic Combinations. Molecules 28. https://doi.org/10.3390/molecules28145299.

Gu, K., Feng, S., Zhang, X., Peng, Y., Sun, P., Liu, W., Yi, Wu., Yun, Yu., Liu, X., Liu, X., Deng, G., Zheng, J., Li, B.o., Zhao, L., 2024. Deciphering the antifungal mechanism and functional components of cinnamomum cassia essential oil against candida albicans through integration of network-based metabolomics and pharmacology, the greedy algorithm, and molecular docking. J. Ethnopharmacol. 319, 117156 https://doi.org/10.1016/j.jep.2023.117156.

Gülçin, İ., 2012. Antioxidant activity of food constituents: an overview. Arch. Toxicol. 86 (3), 345–391. https://doi.org/10.1007/s00204-011-0774-2.

Jažo, Zvonimir, Mateo Glumac, Ivana Drventić, Ljilja Žilić, Tea Dujmović, Danica Bajić, Marko Vučemilo, Ena Ivić, Sanida Bektić, Goran T. Anačkov, et Mila Radan. 2022. The Essential Oil Composition of Helichrysum Italicum (Roth) G. Don: Influence of Steam, Hydro and Microwave-Assisted Distillation . *Separations* 9(10):280. doi: 10.3390/separations9100280.

Jeddi, M., El Hachlafi, N., El Fadili, M., Benkhaira, N., Al-Mijalli, S.H., Kandsi, F.h., Abdallah, E.M., Ouaritini, Z.B., Bouyahya, A., Lee, L.-H., Zengin, G., Mrabti, H.N., Fikri-Benbrahim, K., 2023. Antimicrobial, antioxidant, α-amylase and α-glucosidase inhibitory activities of a chemically characterized essential oil from lavandula angustifolia mill.,. in vitro and in silico investigations. Biochem. Syst. Ecol. 111, 104731 https://doi.org/10.1016/j.bse.2023.104731.

Jia, C.-Y., Li, J.-Y., Hao, G.-F., Yang, G.-F., 2020. A drug-likeness toolbox facilitates ADMET study in drug discovery. Drug Discov. Today 25 (1), 248–258. https://doi.org/10.1016/j.drudis.2019.10.014.

Kokotkiewicz, Adam, et Maria Luczkiewicz. 2016. Celery (Apium Graveolens Var. Dulce (Mill.) Pers.) Oils . P. 325-38 in *Essential Oils in Food Preservation, Flavor and Safety*. Elsevier.

Lipinski, C.A., 2004. Lead- and drug-like compounds: the rule-of-five revolution. Drug Discov. Today Technol. 1 (4), 337–341. https://doi.org/10.1016/j.ddtec.2004.11.007.

Liu, J., Cheng, C., Zhang, Z., Yang, S., Zhang, X., 2021. Optimization of celery leaf tea processing and the volatile components analysis. J. Food Process. Preserv. 45 (3) https://doi.org/10.1111/jfpp.15253.

Majda, E., Bouchra, L., El, O.F., Abdelhak, B., Noureddine, E., 2020. Application of response surface methodology to optimize the extraction of essential oil from rosmarinus officinalis using microwave-assisted hydrodistillation. J. Appl. Pharm. Sci. https://doi.org/10.7324/JAPS.2021.110115.

Mayouf, N., Charef, N., Saoudi, S., Baghiani, A., Khennouf, S., Arrar, L., 2019. Antioxidant and anti-inflammatory effect of asphodelus microcarpus methanolic extracts. J. Ethnopharmacol. 239, 111914 https://doi.org/10.1016/j.jep.2019.111914.

Modaresi, M., Ghalamkari, G., Jalalizand, A., 2012. The effect of celery (apium graveolens) extract on the reproductive hormones in male mice. APCBEE Proc. 4, 99–104. https://doi.org/10.1016/j.apcbee.2012.11.017.

Moradi, S., Fazlali, A., Hamedi, H., 2018. Microwave-assisted hydro-distillation of essential oil from rosemary. Comparison with Traditional Distillation. 10 (1).

Morris, G.M., Huey, R., Lindstrom, W., Sanner, M.F., Belew, R.K., Goodsell, D.S., Olson, A.J., 2009. AutoDock4 and AutoDockTools4: automated docking with selective receptor flexibility. J. Comput. Chem. 30 (16), 2785–2791. https://doi.org/10.1002/jcc.21256.

Mssillou, Ibrahim, Abdelkrim Agour, Meryem Slighoua, Mohamed Chebaibi, Fatima Ez-Zahra Amrati, Samar Zuhair Alshawwa, Omkulthom Al Kamaly, Abdelfattah El Moussaoui, Badiaa Lyoussi, et Elhoussine Derwich. 2022. Ointment-Based Combination of Dittrichia Viscosa L. and Marrubium Vulgare L. Accelerate Burn Wound Healing . *Pharmaceuticals* 15(3):289. doi: 10.3390/ph15030289.

Munshi, Zaki Ahmed B., Mubarak H. Shaikh, Pravinsing S. Girase, Iqrar Ahmad, Harun Patel, et Bhata R. Chaudhari. 2023. Antibacterial Activity of Novel 1-Cyclopropyl-6,7-Difluoro-8-Methoxy-4-Oxo-1,4-Dihydroquinoline-3-Carbohydrazide Derivatives . *Polycyclic Aromatic Compounds* 1-12. doi: 10.1080/10406638.2023.2220866.

Nagella, P., Ahmad, A., Kim, S.-J., Chung, I.-M., 2012. Chemical Composition, Antioxidant Activity and Larvicidal Effects of Essential Oil from Leaves of *Apium Graveolens*. Immunopharmacol. Immunotoxicol. 34 (2), 205–209. https://doi.org/10.3109/08923973.2011.592534.

Nouioura, Ghizlane, Tayeb Kettani, Meryem Tourabi, Layla Tahiri Elousrouti, Omkulthom Al Kamaly, Samar Zuhair Alshawwa, Abdelaaty A. Shahat, Abdulsalam Alhalmi, Badiaa Lyoussi, et Elhoussine Derwich. 2023. The Protective Potential of Petroselinum Crispum (Mill.) Fuss. on Paracetamol-Induced Hepatio-Renal Toxicity and Antiproteinuric Effect: A Biochemical, Hematological, and Histopathological Study. *Medicina* 59(10):1814. doi: 10.3390/medicina59101814.

Nouioura, Ghizlane, Meryem Tourabi, Asmae El Ghouizi, Mohammed Kara, Amine Assouguem, Asmaa Saleh, Omkulthom Al Kamaly, Faiçal El Ouadrhiri, Badiaa Lyoussi, et El Houssine Derwich. 2023. Optimization of a New Antioxidant Formulation Using a Simplex Lattice Mixture Design of Apium Graveolens L., Coriandrum Sativum L., and Petroselinum Crispum M. Grown in Northern Morocco . *Plants* 12(5):1175. doi: 10.3390/plants12051175.

Rana, A., Negi, P.B., Tripathi, A.H.C., Pal, M., Sahoo, N.G., 2022. Chemical composition, antifungal, antioxidant and cytotoxic potential of apium graveolens L. (Celery) leaves essential oil collected from nainital, Uttarakhand. J. Essential Oil Bearing Plants 25 (4), 844–858. https://doi.org/10.1080/0972060X.2022.2113146.

Re, R., Pellegrini, N., Proteggente, A., Pannala, A., Yang, M., Rice-Evans, C., 1999. Antioxidant activity applying an improved ABTS radical cation decolorization assay. Free Radic. Biol. Med. 26 (9–10), 1231–1237. https://doi.org/10.1016/S0891-5849(98)00315-3.

Saini, R.K., Song, M.-H., Ji-Woo, Yu., Shang, X., Keum, Y.-S., 2021. Phytosterol profiling of apiaceae family seeds spices using GC-MS. Foods 10 (10), 2378. https://doi.org/10.3390/foods10102378.

Sama-ae, I., Pattaranggoon, N.C., Tedasen, A., 2023. In silico prediction of antifungal compounds from natural sources towards lanosterol 14-alpha demethylase (CYP51) using molecular docking and molecular dynamic simulation. J. Mol. Graph. Model. 121, 108435 https://doi.org/10.1016/j.jmgm.2023.108435.

Selli, S., Prost, C., Serot, T., 2009. Odour-active and off-odour components in rainbow trout (oncorhynchus mykiss) extracts obtained by microwave assisted distillation-solvent extraction. Food Chem. 114 (1), 317–322. https://doi.org/10.1016/j.foodchem.2008.09.038.

Sheikh, T.A., Ganie, S.Y., Reshi, M.S., 2023. Phytochemistry, pharmacological properties and medicinal uses of apium leptophyllum: a review. Pharmacogn. Rev. 135–43 https://doi.org/10.5530/097627870185.

Tena, N., Martín, J., Asuero, A.G., 2020. State of the art of anthocyanins: antioxidant activity, sources, bioavailability, and therapeutic effect in human health. Antioxidants 9 (5), 451. https://doi.org/10.3390/antiox9050451.

Thaipong, K., Boonprakob, U., Crosby, K., Cisneros-Zevallos, L., Byrne, D.H., 2006. Comparison of ABTS, DPPH, FRAP, and ORAC Assays for estimating antioxidant activity from guava fruit extracts. J. Food Compos. Anal. 19 (6–7), 669–675. https://doi.org/10.1016/j.jfca.2006.01.003.

Thakre, Archana, Gajanan Zore, Santosh Kodgire, Rubina Kazi, Shradha Mulange1, et Rajendra Patil. 2017. Limonene Inhibits Candida Albicans Growth by Inducing Apoptosis. *Medical Mycology*. doi: 10.1093/mmy/myx074.

Thiam, Abdoulaye, Momar Talla Gueye, Cheikhna Hamala Sanghare, El Hadji Barka Ndiaye, Serigne Mbacké Diop, Papa Seyni Cissokho, Michel Bakar Diop, Ibrahima Ndiaye, et Marie-Laure Fauconnier. 2020. Chemical Composition and Anti-Inflammatory Activity of *Apium Graveolens* Var. Dulce Essential Oils from Senegal . *American Journal of Food Science and Technology* 8(6):226-32. doi: 10.12691/ajfst-8-6-1.

Tohidi, B., Rahimmalek, M., Arzani, A., 2017. Essential oil composition, total phenolic, flavonoid contents, and antioxidant activity of thymus species collected from different regions of Iran. Food Chem. 220, 153–161. https://doi.org/10.1016/j.foodchem.2016.09.203.

Tosun, F., Göger, F., İşcan, G., Kürkçüoğlu, M., Kuran, F.K., Miski, M., 2023. Biological activities of the fruit essential oil, fruit, and root extracts of ferula drudeana korovin, the putative anatolian ecotype of the silphion plant. Plants 12 (4), 830. https://doi.org/10.3390/plants12040830.

Ünal, Mustafa ÜmiT, FiLiZ Uçan, Aysun Şener, et Sadik DiNçer. 2012. Research on Antifungal and Inhibitory Effects of DL-Limonene on Some Yeasts . *Turkish Journal of Agriculture and Forestry*. doi: 10.3906/tar-1104-41.

Zhang, H.-F., Yang, X.-H., Wang, Y., 2011. Microwave assisted extraction of secondary metabolites from plants: current status and future directions. Trends Food Sci. Technol. 22 (12), 672–688. https://doi.org/10.1016/j.tifs.2011.07.003.

Zorga, J., Kunicka-Styczyńska, A., Gruska, R., Śmigielski, K., 2020. Ultrasound-Assisted Hydrodistillation of Essential Oil from Celery Seeds (Apium Graveolens L.). In: And Its Biological and Aroma Profiles. Molecules 25(22):5322. https://doi.org/10.3390/molecules25225322.